Lozano-Torres, B.; Blandez, JF.; Sancenón Galarza, F.; Martínez-Máñez, R. (2021). Chromo-fluorogenic probes for beta-galactosidase detection. Analytical and Bioanalytical Chemistry. 413(9):2361-2388. https://doi.org/10.1007/s00216-020-03111-8

Chromo-fluorogenic probes for β-Galactosidase detection

Beatriz Lozano-Torres,[a,b,c,d] Juan F. Blandez,[a,b,c,d] Félix Sancenón[a,b,c,d,*] and Ramón Martínez-Máñez[a,b,c,d,*]

[a] Instituto Interuniversitario de Investigación de Reconocimiento Molecular y Desarrollo Tecnológico (IDM), Universitat Politècnica de València, Universitat de València. Camino de Vera s/n, 46022-Valencia, Spain.

[b] Unidad Mixta UPV-CIPF de Investigación en Mecanismos de Enfermedades y Nanomedicina, Universitat Politècnica de València, Centro de Investigación Príncipe Felipe, Valencia, Spain.

[c] CIBER de Bioingeniería, Biomateriales y Nanomedicina (CIBER-BBN).

[d] Unidad Mixta de Investigación en Nanomedicina y Sensores. Universitat Politècnica de València, IIS La Fe, Valencia, Spain

* Corresponding authors e-mail: rmaez@qim.upv.es; fsanceno@upvnet.upv.es

Keywords: chromo-fluorogenic probes, β-galactosidase detection, cellular senescence, in vitro and in vivo detection

Abstract

β-Galactosidase (β-Gal) is a widely used enzyme as a reporter gene in the field of molecular biology which hydrolyses the β-galactosides into monosaccharides. β-Gal is an essential enzyme in humans and its deficiency or its overexpression results in several rare diseases. Cellular senescence is probably one of the most relevant physiological disorders that involve β-Gal enzyme. In this review, we assess the progress made to date in the design of molecular-based probes for the detection of β-Gal both *in vitro* and *in vivo*. Most of the reported molecular probes for the detection of β-Gal consist of a galactopyranoside residue attached to a signalling unit through glycosidic bonds. The β-Gal-induced hydrolysis of the glycosidic bonds released the signalling unit with remarkable changes in colour and/or emission. Additional examples based on other approaches are also described. The wide applicability of these probes for the rapid and *in situ* detection of de-regulation β-Gal–related diseases has boosted the research in this fertile field.

1. Introduction

The development of new probes for enzymes detection, as well as evaluate their levels, is currently of great importance in different fields from food control to clinical studies.[1, 2, 3] There are a significant number of clinically relevant enzymes that allow immediate determination of human condition and health for instance the enzymatic activity in the liver.[4] In the same way, many of rare diseases are related with high or deficient levels of enzymes which in most cases stem from genetic problems, such as Fabry's disease (due to a deficiency of α-galactosidase) or Hurler's disease (which presents a deficit of the enzyme α-L-iduronidase).[5]

This critical review examines reported approaches in the chromo-fluorogenic detection of β-galactosidase (β-Gal) enzyme, which has a relevant role in both human and animal physiology and molecular biology. At this respect, low levels of β-Gal have been reported to be related to rare diseases, that affects a small proportion of the population, such as GM1 gangliosidosis,[6] Morquio syndrome or Krabbe disease.[7, 8] On the other hand, β-Gal activity is directly related with cellular senescence and it is overexpressed in many aging-related diseases such as atherosclerosis and cardiovascular disease, cancer, arthritis, cataracts, osteoporosis, type 2 diabetes, hypertension and Alzheimer's disease.[9, 10] Cellular senescence is the process initiated in response to stress and cell damage and is an alternative

route of response to programmed cell death. The first tool to detect senescent cells came from the discovery that senescent cells show high levels of lysosomal *β*-Gal activity.[11, 12] This is known as senescence-associated *β*-galactosidase (SA-*β*-Gal) and it has served as the basis for the design of several chromo-fluorogenic probes (*vide infra*). In fact, chromo-fluorogenic probes are attractive and versatile tools for studying biological systems.[13] It has been widely reviewed that an ideal probe for optical imaging must be uptake by cells rapidly, be highly emissive, nontoxic and selective to the targeted relevant biomolecule.[14, 15, 16, 17] Moreover, the probe should ideally be rapidly eliminated via the urinary tract.[18]

From a chemical point of view, most of the reported molecular probes able to detect *β*-Gal are composed by two subunits, i.e. (i) a *β*-galactose residue as a reactive fragment and (ii) a dye/fluorophore as a signalling moiety. In most cases, both subunits are linked with *O*-glycosidic or *N*-glycosidic covalent bonds or through self-immolative fragments containing one glycosidic linkage.[19, 20] The most common mechanism of action of these probes is related to the fact that when galactose is linked to the selected fluorophore, its absorption or emission at a certain wavelength is drastically reduced. However, in the presence of *β*-Gal enzyme, the glycosidic bond is hydrolysed and the dye is released restoring its emission or changing drastically its colour (which can be observed by the naked eye). Based on this concept, one and two-photon fluorophores (such as fluorescein, coumarin derivatives, quinolines, naphthalimides, etc., *vide infra*) and common-used chromophores (nitrophenol, indigo blue, different metal complexes, etc.) have been used as signalling units. These, or similar probes still to be developed, are expected to be a fundamental instrument for the detection of *β*-Gal enzyme in multiple disorders. However, one of the major obstacles still limiting progress in this research area is the low number of methods to track *β*-Gal enzyme activity in live organisms.

We assess herein the progress made to date in the design of molecular-based probes for *β*-Gal detection *in vitro* and *in vivo*. Moreover, the applicability of these probes is discussed depending on how the enzyme is generated (Table 1). For example, some reported *in vitro* o *in vivo β*-Gal activity studies involve the transfection of either bacterial or mammalian cells with the *lacZ* gene, which encodes bacterial *β*-Gal.[21] By this method, *β*-Gal probes have been tested by comparing *β*-Gal activity detection in non-transfected and *lacZ* transfected cells.[22] A more realistic approach to validate *β*-Gal probes consists of using cell lines with high *β*-Gal activity *per se*, such as cells from dyskeratosis congenita patients and primary ovarian cancer cells, replicative senescent cells, or cells undergoing chemical-induced senescence (See Table 1).[11, 23, 24] We hope this review will help researchers in different fields to design more precise and valuable tools for *β*-Gal imaging as well as early detection of diseases related to *β*-Gal enzyme disorders.

Table 1. Summary of photo-physical features and biological applications of *β*-Gal probes.

	Probe	Solvent	$\lambda_{exc}/\lambda_{em}$	Detection approach	Bio-applications	Reference
Solution	**1**	0.02 M Na_2HPO_4, pH 7.2,	400/490	Turn on	Comercial kit	25
	2, 3	100 mM Na_2HPO_4,pH 7.4,	-	Chromogenic (shift from 450 to 490)	-	26
	4	0.15M glycine buffer, pH 7.0 to pH 10.3	365/455	Turn on	Comercial kit	27
	5	100 mM Na_2HPO_4,pH 7.4,	360/460	Turn on	-	28
	6	DMSO/PBS 1:300	365/440	Turn on	-	29
	7	100 mM Na_2HPO_4,pH 7.3	-	Chromogenic (colorless to yellow)	Comercial kit	30
	8	0.1M TRIS, pH 7.0	630/670	Turn on	-	31
	9	50 mM Na_2HPO_4,pH 8.0	-	Chromogenic (shift from 438 to 634)	-	32
	10	PBS	360/↓430↑588	Ratiometric	-	33
	11 to 15	citric acid-phosphoric, pH 4.5	352/503 to 594	Turn on (precipitates)	-	34
	irradiated TMB-1	10.0 mM Tris-HCl buffer, pH = 7.4	-	Chromogenic (colorless to blue)	-	35
	16	PBS	590/610	Turn on	-	36

		17 to 22	DMF/PBS	-	Chromogenic (coloured precipitates)	Comercial kit	37
		23	PBS	-	Chromogenic (colorless to red)	-	38
		24-CuNCs	HEPES buffer, pH 7.4	410/640	Turn off (aggregates)	-	39
		24-GQDs	PBS	370/475	Turn off (inner filter effect)	-	40
		25-Fe^{3+}	HEPES buffer, pH 7.3	-	Chromogenic (colorless to red)	-	41
Chromo-fluorogenic probes for tracking β-Gal activity in vitro	LacZ transfection	**26**	PBS/DMSO	488/550	Turn on	GP293-lacZ	42
		27	PBS (10 mM, pH 7.4)	400/↓515↑460	Ratiometric	HEK293-lacZ	43
		28	PBS (10 mM, pH 7.4)	488/520	Turn on	HEK293-lacZ	44
		29	PBS (10 mM, pH 7.4)	582/601	Turn on	HEK293-lacZ	45
		30	PBS (10 mM, pH 7.4)	525/550	Turn on	HEK293-lacZ	46
		31	PBS (0.2 M , pH 7.4)	501/525	Turn on	HEK293-lacZ	47
		32	PBS (pH 7.4)	525/560	Turn on	HEK293-lacZ, Drosophila melanogaster, Cp211-lacZ and AT1a-lacZ mice tissues.	48
		33, 34	HBSS buffer	570/680	Turn on	C6-lacZ	49
		35	PBS (10 mM, pH 7.4)	405/545	Turn on	C6-lacZ	50
		36	HBSS buffer	640/680	Turn on	HCT116-lacZ	51
		37-39	HEPES (pH 7.3)–DMSO 99.9:0.01 v/v	555/582	Turn on	COS-7-lacZ	52
		40	PBS-EtOH/10:1	375/↓450↑540	Ratiometric (Two-photon)	HEK293-lacZ	53
		41	PBS	430/550	Turn on	HeLa, HepG and HCT-116 + β-Gal (1 U)	54
	cell lines with high β-Gal activity per se	**42**	PBS	344/512	Turn on	OVCAR-3	57
		43	H_2O-THF 99:1	333/495	Turn on (aggregates)	OVCAR-3	58
		44	PBS (20 mM, pH 4.6)	420/565	Turn on (aggregates)	SKOV-3	59
		45	PBS	488/560	Turn on (Two-photon)	SKOV-3	60
		46	PBS	350/↓450↑550	Ratiometric (Two-photon)	OVCAR-3	61
		47	PBS/DMSO 7:3 (50 mM, pH = 7.4)	460/650	Turn on (aggregates)	OVCAR-3	62
		48	PBS (10 mM, pH 7.4)	410/↓580↑650	Ratiometric	OVCAR-3	63
		49	PBS/DMSO 99/1 (0.05 M, pH 7.4)	420/↓490↑530	Ratiometric	SKOV-3	64
		50	HEPES	420/500	Turn on	OVCAR-3, HEK293T-lac Z	65
		51	PBS (10 mM, pH 7.4)	363/↓453↑540	Ratiometric	HT-29, HTC-116, RKO, HCT 116 -lacZ	66
		52	HEPES/ACN 1:4 (10 Mm, pH 7.3)	435/554	Turn on	OVCAR-3	67
		53	PBS/DMSO	690/720	Turn on	SKOV-3	68
		54	DMSO/PBS 4:6 (pH 7)	550/675	Turn on	SKOV-3	69
		55	PBS/DMSO 3.5:6.5 (pH 7.5)	600/640	Turn on	SKOV-3, zebrafish	70
		56	H_2O-THF	356/↓405↑530	Ratiometric	SKOV-3	71
		24-β-CD-CQDs	PBS (10 mM, pH 7.4)	365/445	Turn off	OVCAR	72
		57	PBS (10 mM, pH 7.4)	355/460	Turn on (luminiscent)	SKOV3, OVCAR3	73
		58, 59	H_2O -Ferric ammonium citrate	-	Chromogenic (brown precipitates in presence of Fe^{3+})	Enterobacteriaceae bacteria	74

Fluorogenic probes tracking β-Gal activity in vivo		**60**	H_2O -Ferric ammonium citrate-minium potassium sulfate	-	Chromogenic (violet precipitates in presence of Fe^{3+} or Al^{3+})	E. coli	75
		61a1, 61a2, 62b	0.2 M AcOH–AcONa, pH 5.0	365/580	Blue-green or magenta colour (and a yellow-green fluorescence)	K. pneumonia CMCC 46117	76
		63	PBS buffer (10 mM, pH 7.4, 37 °C)	376/↓461↑540	Ratiometric (Two-photon)	senescent HDF, 26-month-old Sprague−Dawley rat skin tissues	79
		64	PBS/DMSO 99,5:0.5 (pH 7.4)	620/703	Turn on	senescent HDF induced by H_2O_2	80
		65a to 65d	PBS/DMSO 80:20 (pH 7.4)	380/525	Turn on	senescent A375, HT-29 cells induced by hydroxyurea	81
		66	HEPES-DMSO 99.5:0.5	495/545	Turn on	senescent HUVEC induced by H_2O_2	82
		67, 68	PBS buffer (10 mM, pH 7.4, 37 °C)	415/454	Turn on	CT26.CL25, HEK293-LacZ, senescent HeLa induced by camptothecin	83
		69	PBS-DMSO 9:1	488/706	Turn on	senescent MRC5 cells induced by H2O2, and senescent A549 HepG2 induced by MLN4924	84
		70	PBS (pH 7)	356/508	Turn on	senescent HeLa induced by H_2O_2 or by doxorubicin	85
	LacZ transfection	**71**	PBS (pH 9.0)	453/518	Turn on	HEK293 cells expressing β-Gal, SHIN3 xenografted mice	88
		72	PBS/DMSO 7:3 (pH = 7.4)	450/↓500↑685	Ratiometric	293T-LacZ, OVCAR-3, LoVo xenografted mice-avidin-β-Gal	89
		73	DMSO/PBS 1:1	Probe 73: 465/608 Hydrolised probe 73: 646/659	Ratiometric	9L-lacZ, Gli36-lacZ xenografted mice	90
		74	-	-	Bioluminescent	C2C12-LacZ-Luciferase, BALB/c nude mice injected with C2C12-LacZ-Luciferase	91
		75	PBS/TRIS 0.1:2 (pH 7.4)	645/660	Turn on	HEK293-LacZ, ICR mice injected with pCMV-lacZ-targeting the liver	92
		76	PBS/DMSO 99.7/0.3 (pH 7.4)	395/↓440↑545	Ratiometric (Two-photon)	C6-lacZ, U-87 MG xenografted nude mice transfected with pCMV-lacZ	93
		77	PBS (pH 7.4)	580/↓615↑665	Ratiometric	HepG2 cells (ASGPR positive), HepG2-lacZ, HepG2-lacZ xenografted mice	94
		78a, 78b	PBS/DMSO 95/5 (pH 7.4)	400/540	Turn on	CT26-LacZ, CT26-LacZ xenografted mice	96
		79	PBS/DMSO 1/1 (pH 7.4)	530/↓575↑730	Ratiometric	SKOV-3, mice bearing A549 orthotopic tumor injected with β-Gal	97
	cell lines with high β-Gal activity per se	**80**	PBS/DMSO 99.7:0.3 (pH 7.4)	498/550	Turn on	SHIN3, SKOV3, OVK18, OVCAR3, OVCAR4, OVCAR5, OVCAR8, HUVEC, mice model of peritoneal metastasis	98
		81a, 81b	HEPES/DMSO 95:5 (100mM, pH 7.4)	680/ 720, 712	Turn on	SKOV3, SKOV3 xenografted mice	99
		82	PBS (0.1M, pH7.4)	550/↓590↑638	Ratiometric (Two-photon)	OVCAR-3, OVCAR-3 xenografted mice	100
		83	PBS/DMSO 99.9:0.1, pH 4.5	405/540	Turn on (Two-photon)	senescent SK-Mel-103 induced with Palbociclib, Palbociclib treated SK-Mel-103 xenografted nude mice	101
		GOS-NPs	H_2O pH 7.5	546/580	Rhodamine B release	DC1787, X-DC 1774 and X-DC4646	23

GalNP(NB)	H_2O/DMSO 99:1 (pH 4.5)	635/666	NB release/turn on	senescent 4T1 induced with Palbociclib, Palbociclib treated 4T1 xenografted BALB/cByJ mice	104
84	PBS	680/708	Turn on	CT26.CL25, senescent HeLa and MCF7 induced by camptothecin, CT26.CL25 xenografted mice, Camptothecin treated HeLa xenografted mice	105
85	PBS/DMSO 7:3	488/↓580↑730	Ratiometric (Two-photon)	senescent VSMCs induced with Ang II, ApoE-/- mice pretreated with Ang II (probe 85 is encapsulated inside poly(lactic-co-glycolic) acid nanoparticles)	106
86	PBS (pH 7.4)	675/708	Turn on	CT26.CL25, senescent HeLa induced by camptothecin, Camptothecin treated HeLa xenografted mice	107

2. Chromo-fluorogenic probes for tracking *β*-Gal activity in solution.

Chromo-fluorogenic probes in this section are formed by a galactopyranoside residue linked, through an *O*-glycosidic bond, with selected chromophores or fluorophores (fluorescein derivatives, certain coumarins, quinolones, indoxyl derivatives and acridines). These probes presented absorption bands or low quantum yields when linked to the galactose unit. However, after *β*-Gal-induced hydrolysis of the *O*-glycosidic bond, marked changes in the absorption bands or emission enhancements were observed. The same mechanism was active for probes in which nitrophenyl derivatives were linked with a galactose residue and where the optical response is achieved after interaction of the nitrophenyl derivatives released with copper nanoclusters or with quantum dots.

β-Gal enzyme activity has been investigated for over eighty years. The first studies were based simply on the measurement of the enzymatic activity in solution of previously purified enzyme. Moreover, some chromo-fluorogenic probes were developed for the easy measurement of *β*-Gal activity in solution (**1** to **15** in Chart **1** with their emission and excitation wavelengths summarized in Table 1). Probes **1** to **15** are composed by a *β*-galactose residue as a reactive fragment and a chromophore or fluorophore as a signalling moiety. The sensing protocol of probes **1** to **15** shown in Chart 1 is based on the *β*-Gal-induced hydrolysis of a glycosidic bond.[25,26,27,28,29,30,31,32,33,34] The removal of the saccharide induced the release of the free fluorophore or chromophore accompanied with a revival of its fluorescence, shifts in the emission wavelength or marked colour changes (see Scheme **1a**). Moreover, other reported probes for measuring *β*-Gal activity in solution (irradiated probe **1** in presence of TMB, and **16** to **25**) presented more complex sensing mechanisms. For example, the hydrolysis reaction of probe **1** yield fluorescein which allowed the oxidation of 3,3′,5,5′-tetramethylbenzidine (TMB) into oxTBM under irradiation with visible light from a LED. The formation of oxTBM generates a blue solution (λ_{abs} = 652 nm) that allows detection of *β*-Gal in a linear range from 0.10 to 12.9 μg mL^{-1} with a limit of detection (LOD) of 0.04 μg mL^{-1} (Scheme **1b**).[35] Moreover, the fluorescein core was extensively used by Urano and co-workers, who prepared the probe **16** to detect *β*-Gal activity.[36] PBS solutions of **16** were colourless and nearly non-emissive. However, upon addition of *β*-Gal a strong absorption band at ca. 590 nm and a marked emission fluorescence at ca. 610 nm appeared due to *β*-Gal-induced hydrolysis of **16** that yield the coloured and highly emissive dianionic fluorescein derivative **16a** (see Scheme **1c**). A further colorimetric probe (**17**) for *β*-Gal detection was synthesized by Horwitz and co-workers in 1964.[37] It consisted of galactose linked to a substituted indole. This is a well-known colorimetric probe for the detection of *β*-Gal and is usually known with the name of X-gal. In presence of the enzyme, the galactosyl moiety in **17** is removed giving 5-bromo-4-chloro-3-indolyl residue, which dimerizes spontaneously and is oxidized into the insoluble intensely blue product 5,5'-dibromo-4,4'-dichloro-indigo (**17a**) (See Scheme **1d**). Since X-gal (**17**) was reported, many variants have been synthesised with slight modifications giving final compounds that have different colours in the presence of *β*-Gal (**18**-**22**). All of these derivatives are usually commercialized as *β*-Gal activity kit detection systems. Probe **23** for *β*-Gal is based in the opening of a spirocycle.[38] In the absence of the enzyme, PBS solutions of **23** showed an

absorption band centred at 416 nm that was bathochromically shifted to 526 nm after complete hydrolysis. This bathochromic shift was reflected in a colour change from colourless to red, ascribed to the formation of **23a** (Scheme **1e**). Moreover, emission spectra of **23** (λ_{exc} = 463 nm) showed a highly enhanced emission band centred at c.a. 550 nm after treatment with *β*-Gal.

Chart 1. Structures **1**-**15**.

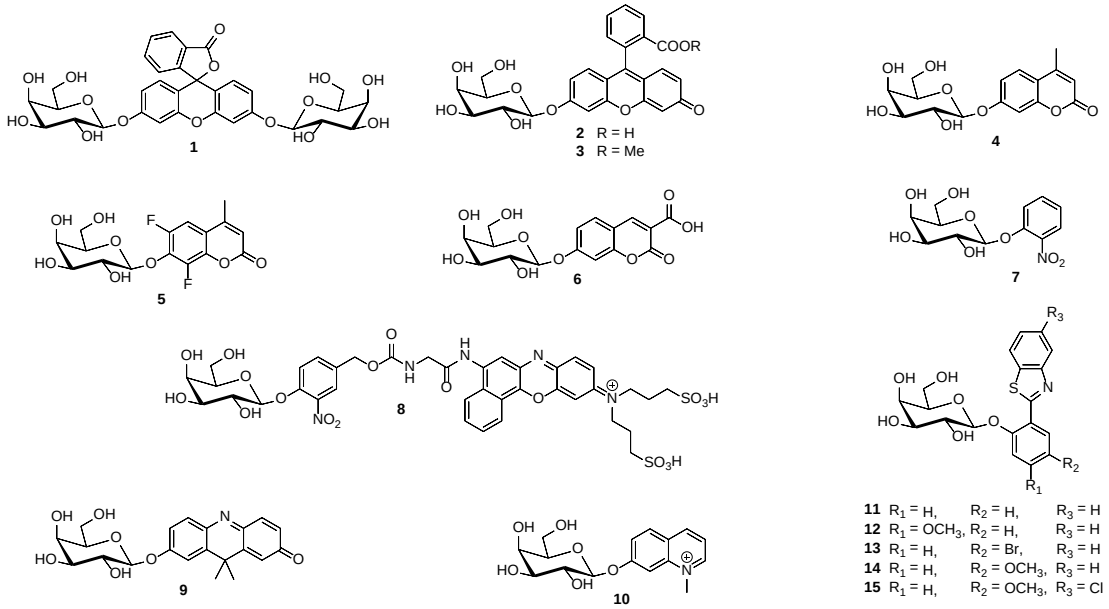

Some other examples have been reported combining molecular probes with copper nanoparticles, quantum dots (QD) or metal complexes (Scheme **2**) for the detection of *β*-Gal activity in solution. For instance, Qian and co-workers recently reported the use of glutathione-protected copper nanoclusters (CuNCs) for *β*-Gal sensing.[39] CuNCs were non-emissive but formed highly fluorescent aggregates (emission at 640 nm upon excitation at 410 nm) in the presence of Al^{3+} cation (Scheme **2a**). In presence of *p*-nitrophenyl-*β*-D-galactopyranoside (**24**) the *β*-Gal enzyme hydrolysed the probe into *p*-nitrophenol which coordinates to the surface of CuNCs aggregates resulting in luminescence quenching (see Scheme **2a**). The fluorescence emission of CuNCs aggregates was also linearly quenched in presence of a constant concentration of **24** and increasing quantities of *β*-Gal. Similarly, Lin et al. used fluorescent quantum dots (GQDs) for the sensitive and selective detection of *β*-Gal activity in presence of **24**. GQDs were fluorescent (λ_{exc}=370nm; λ_{em}=475nm), but in the presence of *β*-Gal and *p*-nitrofenol-*β*-D-galacto-pyranoside (**24**), this emission band was significantly reduced due to the hydrolysis of **24** into p-nitrofenol and subsequent inner filter effect (IFE), see Scheme **2b**.[40] The absorption spectrum of p-nitrophenol overlaps with the excitation spectrum of the GQDs, so that in the presence of the hydrolysate of **24**, a competitive absorption reaction occurs that weakens the excitation of the GQDs causing fluorescence quenching. The system was able to detect *β*-Gal in a range from 20 to 200 U L^{-1} with a detection limit of 4.4 U L^{-1}. In addition, the visual detection of *β*-Gal through in the formation of a complex with strong metal-to-ligand charge transfer (MLCT) bands was assessed by using *p*-aminophenyl-*β*-D-galactopyranoside (**25**) as a substrate of *β*-Gal which is hydrolysed forming *p*-aminophenol.[41] This product can "switch on" the reduction of Fe^{3+} to Fe^{2+}, followed by the complexation of Fe^{2+} with the bathophenanthroline disulfonic acid (BPDS) ligand (See Scheme **2c**) to generate the chromogenic $Fe(BPDS)_3^{4-}$ reporter (**25a**). This leads to the appearance of an intense MLCT absorption band at 535 nm and to a colourless-to-red colour change of the solution. The authors successfully used this approach for the visual detection of *β*-Gal activity in human serum samples.

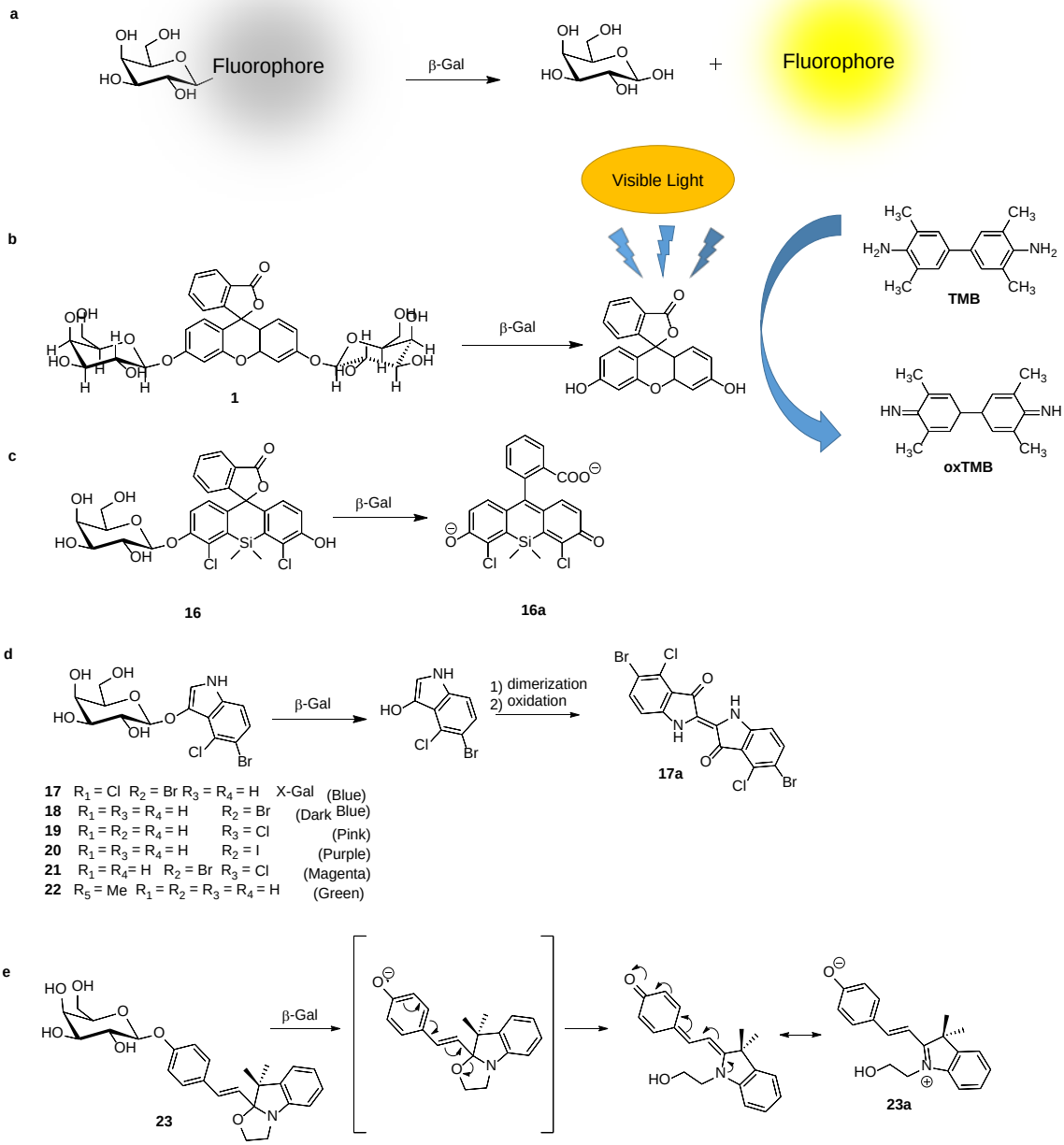

Scheme 1. *β*-Gal probes **16** to **23** and its hydrolysis mechanisms.

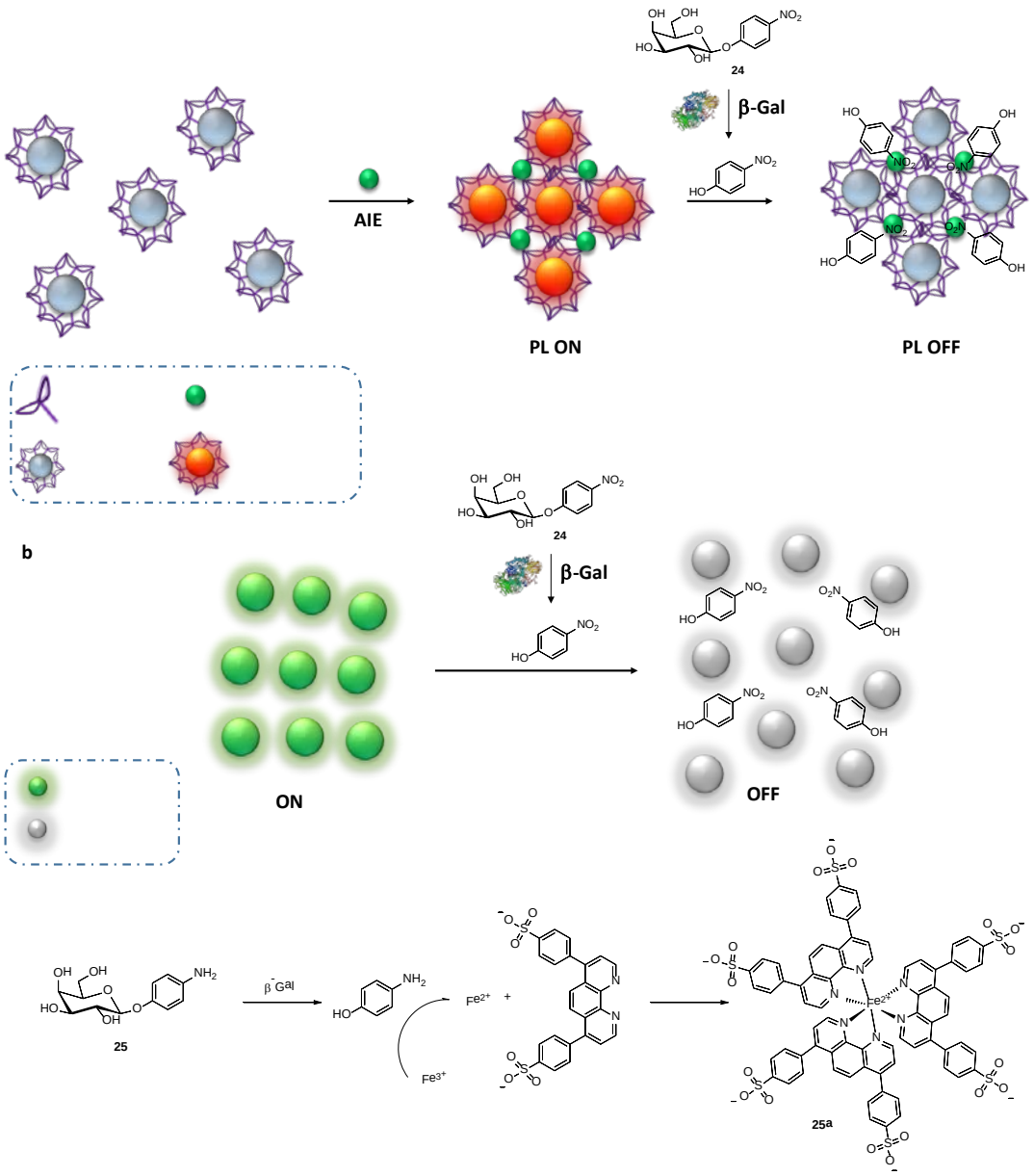

Scheme 2. The sensing mechanism of (a) probe **24** with Cu(NCS), (b) probe **24** with GQDs and (c) probe **25**.

3. Chromo-fluorogenic probes for tracking *β*-Gal activity *in vitro*.

The first attempts to transfer the concepts described above to biological models relied on the development of different probes to detect *β*-Gal activity *in vitro*. For this purpose, researchers tested their probes in two different systems: (i) in cells transfected with the *lacZ* gene which produce bacterial *β*-Gal activity, (ii) using cells that overexpressed *β*-Gal *per se*. Chromo-fluorogenic probes for detection of *β*-Gal activity *in vitro* are also designed linking galactose subunits (which could be additionally acetylated to enhance cellular uptake) to selected fluorophores (fluorescein derivatives, thiazole derivatives, rhodols, luminescent dioxetanes, naphthalimides, tetraphenylethylenes, hemicyanines, quinolines, quinazolinones, luminescent metal complexes) through *O*-glycosidic bonds. In certain examples, a self-immolative fragment connected the galactose residue with the fluorophore.

As cited above, we first will summarize probes that have been applied for *in vitro* studies of *β*-Gal activity involving the transfection of either bacterial or mammalian cells with the *lacZ* gene, which encodes for bacterial *β*-Gal (probes **26**-**41** in Chart **2**). With this method, the *β*-Gal probes can be easily tested *in vitro* by comparing the response in non-transfected and *lacZ* transfected cells. For instance,

Nagano, Urano and co-workers developed several probes for *β*-Gal detection. 2-Me Tokyo Green was used as a fluorophore for the synthesis of **26**,[42] a probe which displayed a clear fluorescent signal in GP293 cells transfected with LNCX2-*lacZ*, whereas in the case of GP293 control cells no fluorescence was observed. Probe **27** consisted on a galactopyranosyl moiety linked, through a self immolative linker, to 7-hydroxycoumarin (donor) and fluorescein (acceptor) as fluorophores able to display a FRET (Förster resonance energy transfer) process.[43] In the presence of *β*-Gal enzyme, fluorescein was removed and FRET efficiency decreases, changing the emission wavelength from 515 to 460 nm (Scheme **3a**). Finally, the emission of 7-hydroxycoumarin was clearly observed in *lacZ* positive cells (due to *β*-Gal hydrolysis of **27**) while it was not apparent in *lacZ*-negative cells, after microinjection of the probe, in the ratiometric images of HEK293 and HEK293-*lacZ* transfected cells. Phenyl-thiazole orange derivative, a widely used dye for marking nucleic acids, linked to a galactose moiety yielded non-emissive probe **28**.[44] As with probe **27**, the authors found bright fluorescent images for *lacZ* positive HEK293 cells treated with **28**, whereas in the case of non-transfected HEK293 cells only a weak emission was detected. Probe **29**, composed by TokyoMagenta linked with a galactose unit, was weakly emissive when excited at 582 nm whereas a new intense emission at 600 nm appeared in presence of *β*-Gal. Also, when control HEK293 cells or transfected with *lacZ* gene were treated with **29** a large fluorescence signal was observed for *lacZ* positive cells compared with control cells.[45]

In another example, Urano et al developed the spirocyclized rhodol derivative **30**. PBS solutions of **30** were nearly non-emissive (quantum yield of 0.009) upon excitation at 525 nm, whereas a marked 76-fold enhancement in the emission intensity in the presence of *β*-Gal was found (quantum yield of 0.141), ascribed to the hydrolysis of the glycosidic bond in **30** that yielded the open fluorophore shown in Scheme **3b**.[46] Besides, **30** was able to visualize *β*-Gal activity in HEK293-*LacZ* cells while no response was observed in HEK293 cells. The enzymatically generated fluorophore (Scheme **3b**) accumulated mainly in the endoplasmic reticule and partially in the Golgi apparatus. The authors also synthesized non-emissive (due to its spirocyclic structure) rhodamine-based probe **31** which was activated (emission at 540 nm) in the presence of *β*-Gal. *In vitro* experiments with **31** showed a marked fluorescence increase in HEK293-*lacZ* cells, while there was no obvious enhancement in HEK293 cells which do not overexpress *β*-Gal.[47] Urano et al developed probe **32** for labelling cells in culture and tissues.[48] PBS (pH 7.4) solutions of **32** were almost non-emissive, however, the addition of *β*-Gal enzyme induced the appearance of a highly fluorescent band centred at 560 nm (λ_{exc}=525 nm), ascribed to the *β*-Gal-induced hydrolysis of **32** that yielded the quinone methide derivative **32a** (Scheme **3c**). Moreover, HEK293-*lacZ* cells incubated with **32** showed a marked fluorescence signal in confocal microscopy studies, that was retained after washing or cell fixation due to the hydrolysis of the probe, formation of quinone methide **32a** and subsequent chemical fixation of this reactive with cell proteins containing nucleophile to give **32b** (see Scheme **3c**). On the contrary, HEK293 cells showed no fluorescence upon incubation with **32**. Finally, **32** was successfully used for detection of *ex vivo lacZ*-induced *β*-Gal activity in *Drosophila melanogaster* and in *Cp211-lacZ* and *AT1a-lacZ* mice tissues.

Tung and co-workers developed two cyanine derivatives **33** and **34** connected with a *β*-galactopyranosil moiety through a self immolative linker.[49] In presence of *β*-Gal, the galactosyl residue was removed which promoted the rearrangement and subsequent elimination of the self-immolative linker, finally yielding 4-methylenecyclohexa-2,5-dienone and **33a** resulting in a strong emission revival at 680 nm (see Scheme **3d**). Intracellular *β*-Gal could not be detected using **33** because the probe was highly hydrophilic being unable to pass through the cell membrane. For this reason, **34** (with an acetylated galactose unit) was selected for confocal studies in C6 and C6-*lacZ* cell lines. In this case, a marked emission was found for C6-*lacZ* cells. The emission obtained using probe **34** was clearly different from that observed for **33**. The authors ascribed this changes to the fact that probe **34** suffered, after cell internalization, a Michael addition with thiols that yielded an intermediate product that suffered a retro-Knoevenagel reaction producing the highly emissive compound **34b** (see Scheme **3e**). Liu et al developed probe **35**, that consists of salicylaldehyde azine functionalized with *β*-galactopyranoside in both *ortho*-hydroxyl groups of the benzene moiety.[50] In the absence of *β*-Gal the probe was non-emissive, whereas in presence of the enzyme an intense fluorescence band at 545 nm appeared due to the enhancement of planarity ascribed to the formation of hydrogen bonding interactions between N, H and O atoms (see **35a** in Scheme **3f**). The probe was investigated in HeLa cells as control and C6-*lacZ* transfected cells which

overexpressed *β*-Gal. For HeLa cells treated with **35,** no emission was observed, whereas for C6-*lacZ* a bright fluorescent image was captured when excited at 405 nm.

In a more complex protocol, the 1,2-dioxetane derivative **36** was used for visualizing endogenous *β*-Gal activity through a chemically initiated electron exchange luminescence (CIEEL) process.[51] In a first step, the response of **36** was tested in plate wells containing the probe, biotinylated *β*-Gal and streptavidin-conjugated Alexa Fluor 647. Biotinylated *β*-Gal induced the hydrolysis of **36** yielding **36a** that decomposes to produce the high-energy intermediate **36b** (see Scheme **3g**). As biotin-streptavidin complex brought both moieties in close proximity, the Alexa Fluor 647 form a CIEEL energy transfer complex with **36b** that emits a red luminescence at 680 nm. Probe **36** was used to detect *β*-Gal activity in HCT116-*lacZ* human colon cancer cells. For this purpose, cells were stained with dialkylcarbocyanine dyes **36c** and **36d** (see Scheme **3g**) and then incubated with **36**. The *β*-Gal overexpressed in HCT116-l*acZ* cells induced the hydrolysis of **36** yielding the high-energy intermediate **36b** which formed emissive energy transfer complexes with dyes **36c** and **36d**.

Chart 2. Structures **26**-**41**.

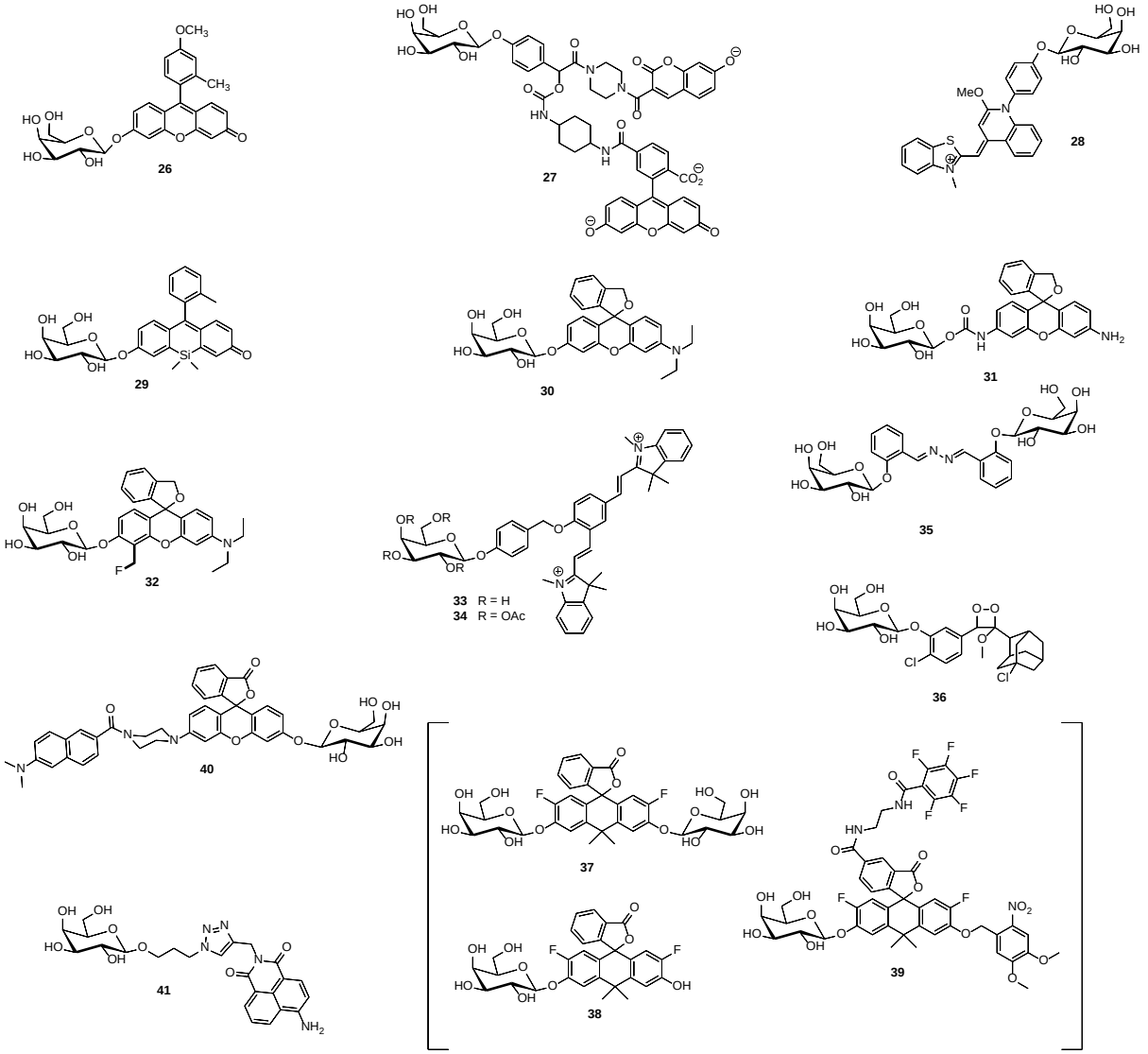

Probes (**37**-**39**) are based on fluorescein derivative Virginia orange.[52] Upon excitation at 555 nm of HEPES (pH 7.3)–DMSO 99.9:0.01 v/v solutions of probes **37** and **38** a very weak emission at 582 nm was found. However, a marked emission enhancement at 582 nm was observed for both molecules in the presence of *β*-Gal. Besides, two-input probe **39**, containing a *β*-Gal active site and a UV-sensible

moiety, was also prepared. **39** was incubated with COS-7 cells and with COS-7 cells transfected with *lacZ* and confocal images showed marked emission intensity enhancements only in *lacZ* positive COS-7 cells upon excitation of 405 nm.

40, a ratiometric two-photon probe, was applied for the detection of *β*-Gal activity in living cells and tumor tissues.[53] In presence of *β*-Gal enzyme, the absorption band of **40** at 450 nm was red-shifted to 510 nm, also a new strong emission band at 540 nm appeared. The intensity ratio value increased by 40-fold for concentration from 0 to 25 U L^{-1} of *β*-Gal and the selectivity of **40** for the enzyme was demonstrated after incubation of the probe with 20 different interfering substances. Hek293 cells were transfected with *lacZ* in order to overexpress *β*-Gal. Two-photon confocal images revealed an intense fluorescent signal for Hek293-*lacZ* in the red channel (λ_{exc}=740nm; λ_{em}=490–600 nm) when compared to the weak signal for control Hek293 cells in the green channel (λ_{exc}=740nm; λ_{em}=420–480 nm). The intense fluorescent signal in the red channel was totally quenched when cells were pre-treated with the *β*-Gal inhibitor D-galactose. Finally, the author proved the ability of probe **40** to monitor *β*-Gal activity in *lacZ* transfected tumors, observing an intense fluorescent signal in the green channel for control tumors and an intense fluorescent signal in the red channel for *lacZ* transfected tumors. Moreover, images of tissues at different depth penetrations demonstrated the advantage of two-photon excitation for tissue imaging.

A common drawback of using *lacZ* gene transfection for the detection of cellular senescence is the fact that this procedure results in high levels of bacterial *β*-Gal expression in the cell cytoplasm, unlike the lysosomal *β*-Gal activity for instance associated with senescent cells (*vide infra*).

Finally, the naphthalimide based probe **41**, which showed a weak emission band at 550 nm (λ_{exc}=430 nm), was validated for measuring *β*-Gal artificially added to cell cultures.[54] Addition of *β*-Gal to PBS solutions of **41** induced a marked emission enhancement at 550 nm due to *β*-Gal-mediated hydrolysis of the glycosidic bond with subsequent release of an emissive naphthalimide derivative. Besides, the response of **41** was tested with HeLa, HepG and HCT-116 cell lines (3 h incubation with **41** and then 1.5 h with *β*-Gal (1 U)). A marked green naphthalimide emission was observed for all three cell lines indicating the cellular uptake of the fluorophore.

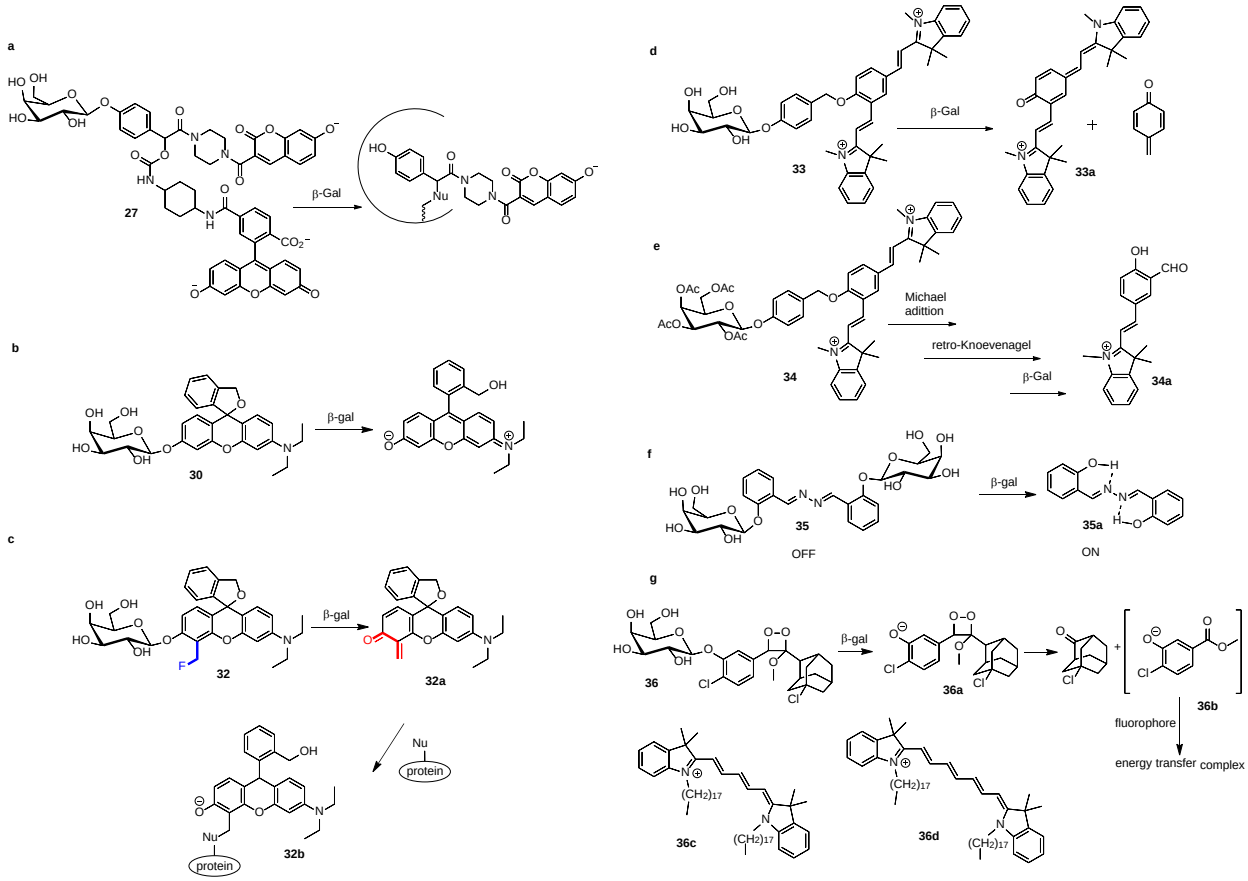

Scheme 3. Hydrolysis mechanism of probes **27**, **30**, **32**, **33**, **34**, **35** and **36**.

β-Gal probes have also been studied in cell lines with high *β*-Gal activity *per se*, such as cells from dyskeratosis congenita patients,[55] primary ovarian cancers,[56] senescent cells, or cells undergoing chemical-induced premature senescence.[11] The lysosomal *β*-Gal enzymatic activity found in these cells seems a better approach for the diagnosis and clinical analysis of diseases associated with dysregulation of the enzyme. Besides, in these cells, the *β*-Gal activity is located in the lysosomes where for the *lacZ* transfected cells the enzyme is mainly detected in the cytosol. Probes used for *β*-Gal enzymatic detection in dyskeratosis congenita, primary ovarian cancer and senescent cells are described below (structures **42**-**62** in Chart **3** and **63**-**70** in Chart **4**).

Ovarian cancer cell lines and some colon cancer cells together with cells from dyskeratosis congenita patients have been widely used as biological models to test *β*-Gal probes. These kinds of cells present abnormal high levels of *β*-Gal. *β*-Gal detection in OVCAR-3, through an aggregation-induced emission (AIE) protocol, using probe **42** (composed by a *β*-galactosyl reactive residue linked with a tetraphenylethylene derivative) was assessed.[57] PBS solutions of **42** showed negligible fluorescence upon excitation at 344 nm. However, upon incubation with *β*-Gal enzyme, a marked emission enhancement at 512 nm was found. The observed emission enhancement was ascribed to the enzymatic hydrolysis of the *β*-galactosyl moiety that yielded a tetraphenylethylene derivative which had poor water solubility forming highly emissive aggregates (LOD of 0.33 U mL^{-1}). Probe **42** was tested in HeLa cells as control and in OVCAR-3 (which overexpress endogenous *β*-Gal) cells. As expected negligible emission was observed in HeLa and a marked green fluorescence was seen in OVCAR-3 cells. Another example of an AIE sensor is probe **43**, which features a hydroxyphenylquinazolinone skeleton bound to galactose. Probe **43** has a very low fluorescence due to the presence of galactose that disrupted the formation of intramolecular hydrogen bonds in water-THF 99:1 v/v solution. However, once galactose unit of **43** is released in the presence of the enzyme, a marked emission at 495 nm (λ_{exc}=333 nm) was observed due to the formation of aggregates (Scheme **4a**). Probe **43** shows a detection limit of 0.013 $U \cdot mL^{-1}$. Besides, **43** was not toxic for OVCAR-3 cells and allowed the detection of *β*-Gal by confocal images. In addition, the fluorescence signal increased when OVCAR-3 cells were incubated with exogenous *β*-Gal and this signal decreased in the presence of D-galactose, a *β*-Gal inhibitor.[58]

Chart 3. Structures **42**-**62**.

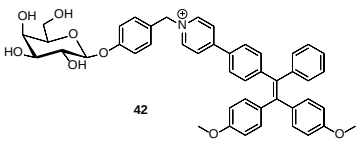

42

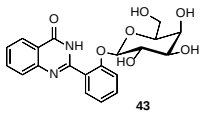

43

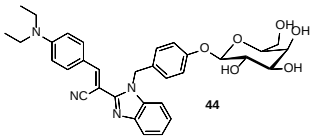

44

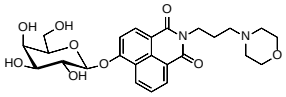

45

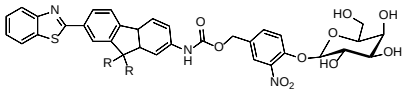

R= $CH_2CH_2OCH_2CH_2OCH_3$

46

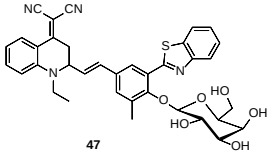

47

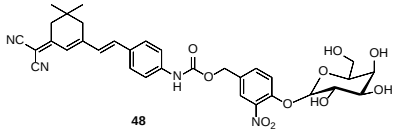

48

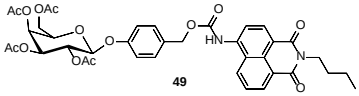

49

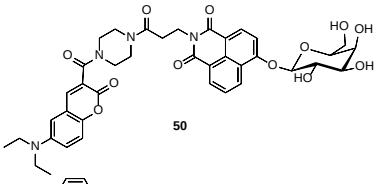

50

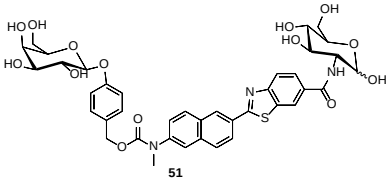

51

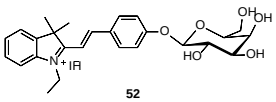

52

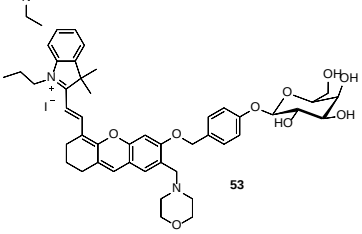

53

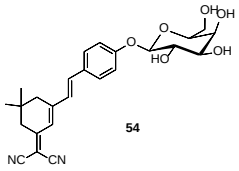

54

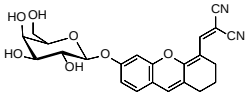

55

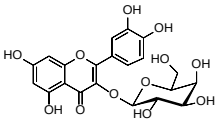

56

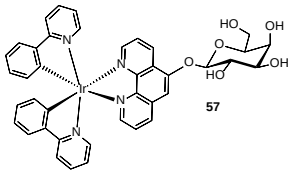

57

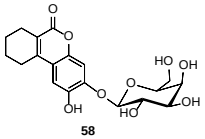

58

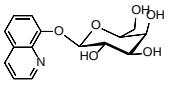

59

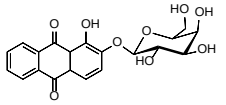

60

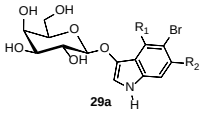

29a

61a$_1$ R_1=Cl, R_2=H
61a$_2$ R_1=H, R_2=Cl

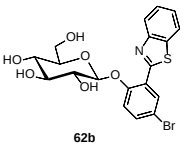

62b

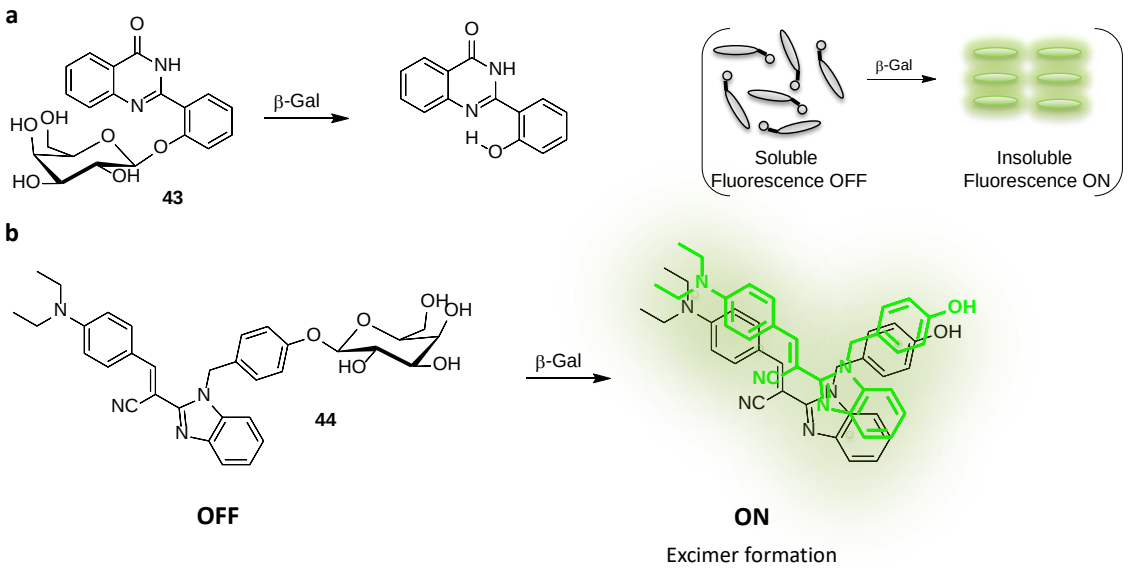

Scheme 4. Mechanism of *β*-Gal detection using (a) probe **43** and (b) probe **44**.

Similarly, a cyanovinylene-based fluorescent probe with excimer emission features for monitoring *β*-Gal activity was recently developed.[59] Probe **44** is non-emissive from 500 to 650 nm due to the galactopyranose moiety in its structure, which promote the dispersion of the molecules in water and serves also as recognition group. However, *β*-Gal enzyme triggers the formation of aggregates (Scheme **4b**) with the subsequent apparition of a strong fluorescent red-shifted band at 565 nm (λ_{exc}=420 nm) with a LOD of 0.17 U. These aggregates were easily dissolved by adding organic solvents. After total characterization of **44**'s spectroscopic properties, SKOV-3 cells were used as a biological model to imaging endogenous *β*-Gal. SKOV-3 cells did not present any noticeable autofluorescence whereas, after incubation with **44**, showed a moderate green fluorescent signal. Moreover, pre-treatment of cells with the *β*-Gal inhibitor D-galactose gave very weak fluorescent images. Only as a proof of concept, SKOV-3 cells were treated with hydroxyurea, a senescence inducer, and incubated with **44**, obtaining strong fluorescent images due to the high levels of *β*-Gal. Finally, co-localization experiments with lysosome indicator LTR99, confirmed the subcellular location of the enzyme in the lysosomes.

Probe **45** used a naphthalimide fluorophore, which was additionally functionalized with a morpholino moiety for lysosomal targeting.[60] PBS solutions of **45** were non-emissive but a marked fluorescence enhancement at 560 nm in the presence of *β*-Gal enzyme was found. The emission enhancement was due to the enzyme-induced hydrolysis of the glycosidic bond in **45** that released a naphthalimide fluorophore (LOD of 4.0 x 10^{-5} U mL^{-1}). One- (excitation at 488 nm) and two-photon (excitation at 750 nm) microscopy studies, carried out with **45** in L-02 (human normal hepatic), BEL-7402 (human hepatocellular carcinoma) and SKOV-3 (human ovary carcinoma) cell lines, showed only a marked emission in the later which overexpress *β*-Gal. The ratiometric probe **46**, which consists of a 7-(benzo[d]thiazol-2-yl)-9,9-bis(2-(2-methoxyethoxy)ethyl)-9H-fluoren-2-amine linked to a galactose though 4-hydroxy-3-nitrobenzyl alcohol, was used for the detection of *β*-gal in living cells. PBS solutions of **46** showed an emission peak at 450 nm, whereas in the presence of *β*-Gal enzyme a new fluorescence at 540 appeared (ascribed to the free fluorophore). F_{550}/F_{450} ratio versus concentration of *β*-gal exhibits a linear change from 0 to 175 U L^{-1} with a detection limit of 0.19 U L^{-1}.[61] In order to corroborate the ability of **46** to detect *β*-Gal in living cells, the authors employed OVCAR-3 cells (positive *β*-Gal) and MDBK as negative control. OVCAR-3 cells incubated with **46** exhibited a marked green fluorescence due to the free fluorophore produced after *β*-Gal-induced hydrolysis of the glycosidic bond in **46**. Probe **47** is formed by a 2-(2-hydroxyphenyl) benzothiazole fluorophore (HTB) linked with a galactose unit.[62] Aqueous solutions of **47** were nearly non-emissive, whereas in the presence of *β*-Gal enzyme a marked

NIR emission at 650 nm was observed. This NIR emission was ascribed to the *β*-Gal-induced hydrolysis of **47**, which produced highly fluorescent aggregates of the insoluble HTB fluorophore. Probe **47** was tested in SKOV-3 (with endogenous *β*-gal) and HeLa cells (negative control). The obtained results showed a marked NIR emission for SKOV-3 cells (due to the formation of aggregates) when compared to the negligible fluorescence observed for HeLa cells. Co-location experiments indicated that fluorophore aggregates were formed into the lysosomes of SKOV-3 cells. Another NIR ratiometric probe (**48**) is formed by the galactose unit linked to an (*E*)-2-(3-(4-aminostyryl)-5,5-dimethylcyclohex-2-en-1-ylidene)malononitrile fluorophore through a self-immolation spacer.[63] PBS solutions of **48** presented an emission band centred at 580 nm that was progressively vanished with the concomitant appearance of a new fluorescence at 650 nm in the presence of *β*-Gal. Fluorescence intensity ratio (F_{650}/F_{580}) displayed a linear fit with the *β*-Gal concentration in the 0–200 U L^{-1} range and a detection limit of 0.86 U L^{-1}. Authors tested **48** in OVCAR-3 cells as positive control and MDBK cells as a negative control. OVCAR-3 cells incubated with **48** showed a marked enhancement in the F_{650}/F_{580} ratio as a consequence of *β*-Gal-induced hydrolysis of the probe. This enhancement was not observed when MDBK were treated with **48** and with OVCAR-3 previously treated with D-galactose (a *β*-Gal inhibitor), demonstrating that the observed emission was due to endogenous *β*-Gal activity. Chen et al described another ratiometric probe (**49**) containing a 4-amino-1,8-napthalic anhydride fluorophore and an acetylated galactose linked through a benzaldehyde linker.[64] PBS solutions of probe **49** presented an emission band at 490 nm whose intensity progressively decreased in the presence of *β*-Gal. Besides, a new emission at 530 appeared ascribed to the free fluorophore. Fluorescence intensity ratio (I_{530}/I_{490}) allowed *β*-Gal visualization with a limit of detection of 1.4×10^{-3} U·mL^{-1}. The ability of **49** for exogenous *β*-Gal detection was assessed using HeLa cells incubated with the probe and then with the enzyme. Besides, endogenous *β*-Gal was detected in SKOV3 cells where the initial blue fluorescence of probe **49** changed to green with time. This change was not observed when SKOV3 cells were incubated with D-galactose.

Another probe for the detection of *β*-Gal enzyme *in vitro* is **50** that contains a coumarin (donor) and napthalimide (acceptor) and galactose linked with the naphtalimide core.[65] HEPES solutions of probe **50** showed the typical coumarin emission at 500 nm (λ_{exc}=420 nm) attributed to a galactose-induced quenching of the emission of the naphthalimide fluorophore through an ICT process. In the presence of *β*-Gal enzyme, the ICT process was inhibited, due to the hydrolysis of the glycosidic bond, with the subsequent activation of a FRET process which induced the appearance of the naphthalimide emission at 570 nm. **50** was used to detect *β*-Gal in OVCAR-3 cells (with endogenous *β*-Gal) and in HEK293T cell transfected with pSV-*β*-Gal. Besides, when the probe was incubated with OVCAR-3 previously treated with D-glucose (*β*-Gal inhibitor) minimal fluorescence was observed.

More recently, a two-photon probe (**51**) with a dual recognition site, which consists of a fluorophore linked to a glucose transporter unit (which increase the uptake in by cancer cells when compared with normal cells) and a galactose unit, has been developed.[66] Addition of increasing quantities of *β*-Gal to PBS solutions of **51** lead to the progressively quenching of a broad emission band centred at 453 nm and the concomitant appearance of a new emission at 540 nm due to the hydrolysis of the glycosidic bond that linked galactose with the fluorophore. The ability of probe **51** to monitor *β*-Gal activity was evaluated in control and *lacZ*-transfected HCT 116 cells, obtaining a ratiometric response from blue for *lacZ (-)* cells to green for *lacZ (+)* cells. Then a normal colon cell line (CDD-18Co) was compared with three colon cancer cell lines (HT-29, HTC-116 and RKO) by two-photon microscopy (TPM). Probe **51** was able to discriminate between cancer cells (with higher *β*-Gal levels) and control. Besides, the intensity of the image was higher depending on the type of cancer cell, allowing also to clearly differentiating the cancer cell lines. Finally, **51** was used to detect colon cancer cells in human colon tissues with three different cancer stages such as normal, adenoma (benign tumor), and carcinoma (malignant tumor). The presence of carcinoma was notably distinguished from adenoma or normal tissue, whereas adenoma was not easily discriminated from normal tissue by two-photon imaging. However, the plot of intensity versus F_{green}/F_{blue} ratio of the TPM images revealed that the stages of normal, adenoma, and carcinoma were clearly discriminated by their area. Hu et al described the synthesis of a colorimetric-fluorescent probe **52**, composed by a merocyanine chromophore linked with a galactose unit.[67] PBS solutions of **52** were non-emissive but a marked emission at 554 nm appeared in the presence of *β*-Gal enzyme due to the hydrolysis of the glycosidic bond in the probe and the subsequent release of a

merocyanine chromophore. A LOD of 0.019 U·mL^{-1} was obtained. Probe **52** was able to detect endogenous *β*-Gal in OVCAR-3 cells, whereas negligible activity was observed in HeLa cells.

A NIR lysosome-targeting probe for *β*-Gal detection was recently developed by Liu and co-workers. The probe **53** is composed by an hemycyanine group, a xantene moiety, a morpholine heterocycle as lysosome-targeting moiety and a galactopyranoside as recognition unit.[68] PBS/DMSO solutions of **53** showed three overlapped bands at 550, 600, and 650 nm, that were 100 nm red-shifted in presence of *β*-Gal. Moreover, **53** was non-emissive in the 700 to 830 nm range (λ_{exc}=690 nm), but after incubation with 2 U mL^{-1} of *β*-Gal, a new intense fluorescent band centred at ca.720 nm appeared. The probe presented good selectivity for *β*-Gal and did not respond to any possible interferents. Then **53** was validated in SKOV-3 cells, showing an ultrafast response from 1 min to 10 min, when the fluorescent signal reaches the maximum intensity. Finally, fluorescent signals in SKOV-3 cells co-localized with lysosome indicator LysoTracker R with a correlation coefficient of 0.83. Another OFF-ON fluorescent probe **54** was recently synthesised by Zhang et al. based on a NIR dicyanoisophorone derivative.[69] UV spectra of **54** showed an absorption band centred at ca. 400 nm, which is bathochromically shifted to 430 nm with the appearance of a new absorption peak at 550 nm, in the presence of *β*-Gal. Moreover, fluorescence emission of DMSO-aqueous solutions of hydrolysed probe changed with the proportion of PBS (max emission in DMSO/PBS 4:6 v/v mixtures), with pH (max emission at pH=7) and with temperatures (max emission at 37ºC), upon excitation at 550 nm (λ_{em}=675 nm). The response of probe **54** was selective for *β*-Gal enzyme in the presence of many diverse interfering species, with a LOD=3.2 x 10^{-3} U. Finally, SKOV-3 cells were incubated with **54**, and bright fluorescent images after 30 min were acquired in sharp contrast to the non-fluorescent images obtained for HepG2 cells (used as control cell line with low levels of *β*-Gal) treated with **54**. In addition, pre-incubated SKOV-3 cells with D-galactose (a *β*-Gal inhibitor) for 1 h treated then with **54**, demonstrated that enzymatic hydrolysis of galactopyranoside moiety triggered the increase in the fluorescent signal.

The same authors developed a xanthene based OFF-ON fluorescent probe **55** for tracking endogenous *β*-Gal in living cells and zebrafish.[70] **55** was non-emissive at 640 nm (λ_{exc}=600 nm), while a remarkable fluorescent band appeared upon addition of increasing quantities of *β*-Gal. Selective response to *β*-Gal compared to interfering species such as other enzymes, aminoacids or cations, was also noticed by the naked eye (aqueous solutions of **55** changed from pink to purple only in presence of *β*-Gal). The maximum fluorescence intensity of the hydrolysed probe was observed at pH 7.5 and in PBS/DMSO 3.5:6.5 v/v solutions. As in the last example, confocal images of SKOV-3 cells incubated with **55** presented an intense fluorescent signal in the red channel (λ_{exc}=514 nm.), whereas SKOV-3 (pre-treated with D-galactose inhibitor) and LO2 and HeLa cells as a control, did not show any noticeably fluorescent signal after treatment with **55** probe. Finally, zebrafish larvae incubated with **55** also presented a tiny fluorescent signal in the ventral part of the body, which disappeared when zebrafish were pre-treated with D-galactose inhibitor. The natural flavonoid hyperoside (quercetin-3-*O*-*β*-galactoside, **56**), isolated from *Hedyotis diffusa*, was used for the imaging of *β*-Gal in living cells.[71] PBS solutions of hyperoside showed a marked emission band at 405 nm (excitation at 356 nm) that was progressively quenched in the presence of *β*-Gal enzyme. Besides, a new emission at 530 nm appeared (reaching its maximum emission after 70 min). This emission band was ascribed to the formation of highly fluorescent quercetin aggregates, generated after enzymatic hydrolysis of hyperoside. From the titration profiles obtained by the addition of increasing amounts of *β*-Gal a limit of detection of 0.013 U mL^{-1} was measured. Besides, hyperoside was able to detect *β*-Gal in the Golgi apparatus and mitochondria in SKOV-3 cells (with endogenous *β*-Gal overexpression).

The two following examples show detection of *β*-Gal using different sensing mechanisms. In the first one, *β*-cyclodextrin functionalized carbon quantum dots (*β*-CD-CQDs) were used for *β*-Gal activity evaluation *in vitro*.[72] The authors monitored *β*-Gal activity using a mixture of *β*-CD-CQDs and 4-nitrophenyl-*β*-D-galactopyranoside (**24**). *β*-Gal is able to hydrolyse the glycosidic bond in **24** releasing *p*-nitrophenol which formed supramolecular inclusion complexes with the grafted *β*-CD. As a consequence, the emission of *β*-CD-CQDs was quenched (Scheme **5a**). *β*-Gal enzyme was detected with a limit of detection as low as 0.6 U L^{-1}. MTT viability assays showed that *β*-CD-CQDs were non-toxic for OVCAR-3 cells. Besides, OVCAR-3 cells incubated with *β*-CD-CQDs showed a marked fluorescence. However, when OVCAR-3 cells were incubated with *β*-CD-CQDs and with **24** a marked emission

quenching was found. The other example used iridium(III)-based long-lived luminescence probe (**57**) for discriminating ovarian carcinoma cell lines from normal cell lines.[73] PBS solutions of **57** showed negligible luminescence, however, luminescence was highly increased after treatment with *β*-Gal. Moreover, the selectivity of the probe was tested by treating **57** with glutathione, cysteine, homocysteine, magnesium ion (Mg^{2+}), adenosine triphosphate, S-adenosyl methionine and bovine serum albumin, and no luminescence response was observed. Finally, confocal images of HUVEC and HEK-293T as control and the overexpressing *β*-Gal SKOV3 and OVCAR3 cells were taken after treated with the probe; fluorescence was only observed in positive *β*-Gal cell lines.

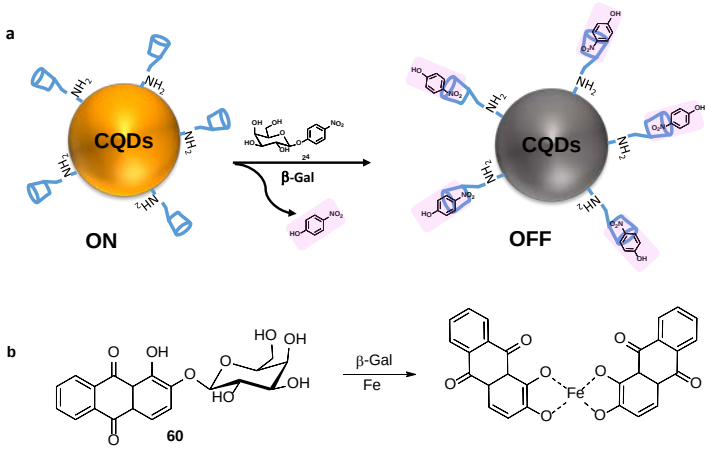

Scheme 5. Mechanism of detection of *β*-Gal using (a) probe **24** and *β*-CD-CQDs and (b) probe **60**.

Furthermore, some strains of bacteria have high levels of *β*-Gal activity per se and have been used to compare different chromogenic probes. In this context, James et al. synthesised probes **58** and **59** based on cyclohexeneesclutin and 8-hydroxyquinoline moieties respectively, for the detection of *β*-Gal and compared them with the X-gal (**17**) kit in different strains of *Enterobacteriaceae*.[74] Products formed after enzymatic hydrolysis conducted to a brown-black complex with ferric ions (present in agar prepared for culture bacteria) giving a clearly visible non-diffusible product. **58** showed similar results as X-Gal for most of the strains. However, **59** did not produce any discernible reaction in some of the positive X-Gal strains. The same authors, described probe **60** consisting of alizarin (1,2-dihydroxyanthraquinone) linked to galactose.[75] When *β*-Gal was present, alizarin was released and formed chelates with a variety of metal ions such as Fe(III) or Al(III) giving bright colours. **60** was tested in colonies of *E. coli* and, when ferric ammonium was present in the media, a bright violet colour appeared, whereas in presence of aluminium, bright red colour was observed (Scheme **5b**). In a similar context, Wu et al synthesised probes **61a**$_1$, **61a**$_2$ and **62b** for the visual detection of foodborne pathogenic bacteria.[76] The authors treated *K. pneumonia* CMCC 46117 bacteria (positive in *β*-glucosidase and *β*-galactosidase activities) and *Salmonella typhimurium* ATCC 14028 (as a negative control) with **61a**$_1$ + **62b** or with **61a**$_2$ + **62b** mixtures. Both mixtures induced the appearance of a blue-green or magenta colour (and a yellow-green fluorescence under 365 nm UV-light) on *K. pneumonia* (as a consequence of probe hydrolysis) without any colour/fluorescence on *S. typhimurium*.

Senescent cells are necessary for the body homeostasis and normally destroy themselves via apoptosis, or are also removed by the immune system. However, upon persistent damage or during aging, when the immune system weakens, senescent cells tend to accumulate in tissues promoting local inflammation, tissue aging and destruction and potentially, tumorigenesis and metastasis.[77] All these issues make early detection of senescent cells a highly appealing and rapidly growing field.[16] The first tool to detect senescent cells came from the discovery that senescent cells show high levels of lysosomal *β*-Gal activity.[11, 78]

Chart 4. Structures **63-70**.

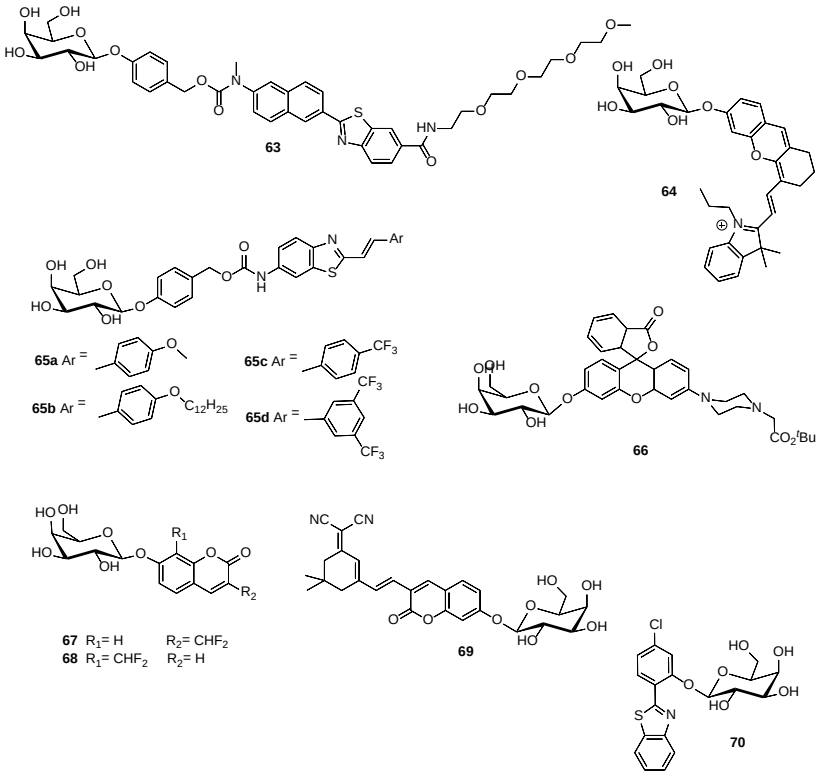

This is known as senescence-associated *β*-galactosidase (SA-*β*-Gal) and it has served as the basis for testing and design of many chromo-fluorogenic probes (probes **63**-**70** in Chart **4**). For instance, Kim et al reported the ratiometric two-photon fluorescent probe **63** composed of 6-(benzo[d]thiazol-2′-yl)-2-(methylamino)-naphthalene as a fluorophore, a self immolative carbamate as a linker, a polyether as solubilizing group and galactose as hydrolytic moiety.[79] The maximum of the emission of **63** changed from 461 to 540 nm in the presence of *β*-Gal, which induced the hydrolysis of galactose in the anomeric carbon with the subsequent rupture of the self immolative linker that released the polyether-functionalized 6-(benzo[d]thiazol-2′-yl)-2-(methylamino)-naphthalene fluorophore. Probe **63** was tested in human diploid fibroblasts (HDF) as a replicative model of senescence from 2 to 20 days. Treating the cells with **63**, the authors observed that the ratio F_{yellow}/F_{blue} increased from 0.30 to 1.13 for 2 days to 20 days passages, respectively when exciting at 750 nm. Finally, the authors used the probe for staining 7-month-old and 26-month-old Sprague−Dawley rat skin tissues, showing an enhancement of F_{yellow}/F_{blue} ratio from 0.55 to 0.78, respectively. PBS solution of **64** presented a weak emission band at 665 nm in the absence of *β*-Gal, whereas in the presence of this enzyme a new emission at 703 nm appeared (12.8-fold enhancement).[80] The authors tested the probe response in a premature senescence model of human diploid fibroblast (HDF) cells induced by H_2O_2. Control and senescent cells were treated with **64**. No signal was observed for control cells, whereas in senescent cells clear turn-on NIR fluorescent images were captured.

Probes **65a-65d** are composed by a 6-aminostyryl-benzothiazole derivative (fluorophore) connected to galactose through a self-immolative benzyl carbamate linker.[81] Among all the prepared probes, **65a** was selected for experiments in cells due to its higher selectivity and lower limit of detection for *β*-Gal (5×10^{-4} U mL^{-1}). PBS solutions of probe **65a** showed negligible fluorescence whereas in the presence of *β*-Gal a marked emission at 525 nm appeared. Probe **65a** was tested in senescent human melanoma A375 and human colorectal adenocarcinoma HT-29 cells, where senescence was achieve using hydroxyurea (HU) as chemical senescence inductor. As expected, a marked fluorescence was observed only in senescent cells as a consequence of *β*-Gal-induced hydrolysis of the probe. Finally, **65a** was used in real-time monitoring of the senescence appearance in A375 cells via time-lapse fluorescence microscopy.

Probe **66**, for the detection of lysosomal *β*-Gal in senescent vascular endothelial cells, is composed of a rhodol skeleton fluorophore linked to galactose unit.[82] HEPES-DMSO 99.5:0.5 v/v solutions of **66** were almost non-emissive, whereas in the presence of *β*-Gal a marked emission at 545 nm

was observed. Detection of endogenous *β*-Gal activity in HUVEC senescent cells (where senescence was induced by the treatment of normal HUVEC cells with H_2O_2) was achieved using probe **66** and confocal microscopy measurements. These studies also showed that probe **66** co-localized with lysosome after 24 h of the treatment. Xie et al. reported **67** (containing a difluoromethyl moiety in 8-position of coumarin) and **68** (an isomer in which the difluoromethyl moiety is located in 3-position of coumarin) probes for *β*-Gal. **68** showed a higher fluorogenic response, improved fluorescent labeling signal, and easier synthesis than **67**.[83] The authors demonstrated these advantages via in-gel fluorescence imaging, observing that **68** emitted stronger fluorescence than **67** in presence of *β*-Gal (as a hydrolytic enzyme) and BSA (as fixating protein). Then, wild type CT26.WT as control and CT26.CL25 (as *β*-Gal expressing) cells were treated with **67** and **68**. As expected, CT26.CL25 cell images presented an enhanced fluorescent signal (higher when treated with probe **68** than when **67** was used) than that observed for CT26.WT. These results were also observed in *lacZ*-transfected HEK293 compared to control HEK293 and also in senescent HeLa cells (which overexpressed *β*-Gal) induced by camptothecin treatment. PBS-DMSO 9:1 v/v solutions of NIR probe **69** showed a very weak emission band at 592 nm (quantum yield of 0.01) when excited at 488 nm.[84] Addition of *β*-Gal enzyme induced the appearance of a red-shifted emission band centred at 706 nm, which was ascribed to the NIR fluorophore generated after enzymatic hydrolysis of probe **69**. From the emission titration profiles, obtained after the addition of increasing amounts of *β*-Gal enzyme, a limit of detection of 0.0015 U mL^{-1} was determined. The probe was tested in normal and senescent MRC5 cells (in which senescence was induced with H_2O_2) and only in the senescent cells, a marked emission in the red channel was observed. The same results were obtained with normal and senescent A549 and HepG2 cells (senescence was induced by administration of MLN4924, an anticancer agent that promoted senescence in tumors). Finally, Mizuta and co-workers prepared probe **70**, based on 2-(2'-hydroxyphenyl)benzothiazole fluorophore, for the measurement of *β*-Gal activity in senescent cells.[85] PBS solutions of probe **70** showed negligible fluorescence when excited at 356 nm (quantum yield of 0.045), whereas a marked emission band at 508 nm (quantum yield of 0.339) was formed in the presence of *β*-Gal enzyme. This marked emission enhancement was ascribed to the enzymatic hydrolysis of probe **70**, which generated a highly emissive 2-(2'-hydroxyphenyl)benzothiazole fluorophore. On the other hand, probe **70** was successfully used to detect *β*-Gal activity in senescent HeLa cells in which senescence was generated by treatment with H_2O_2 or with doxorubicin administration.

4. Fluorogenic probes tracking *β*-Gal activity *in vivo*

The potential ability of some probes to detect *β*-Gal activity *in vivo* has also been studied. In these *in vivo* models *β*-Gal activity overexpression has been achieved using different protocols: (i) labelling tumour cells with avidin-*β*-Gal conjugate, (ii) transfecting cells with *lacZ* in the same manner as *in vitro* studies detailed above, (iii) using mice with cells that overexpress *β*-Gal *per se* or (iv) mice containing senescent cells. Most of the probes tracking *β*-Gal activity *in vivo* are composed by a galactopyranoside subunit linked, through *N*- or *O*-glycosidic bonds, to selected fluorophores (fluorescein derivatives, BODIPYs, naphthalimides, squarylium derivatives, luminescent 1,2-dioxetanes, acridinones, rhodols, rhodamine derivatives, hemicyanines). Interestingly some NIR and two-photon dyes have also been used. Some concepts using nanotechnology for *β*-Gal activity detection *in vivo* are also described below.

Avidin-*β*-Gal is an enzyme-conjugate that have been used to localize *β*-Gal activity in cancer cells.[86, 87] Avidin has a high affinity for lectins expressed on the surface of different cancer cell lines. Hereby, avidin-*β*-Gal conjugate preferentially binds to the surface of this type of tumors. Probes **71** and **72** in Chart **5** were used to detect avidin-*β*-Gal. Another common method to introduce *β*-Gal activity in tumors is the use of *lacZ* gene, as explained above for *in vitro* studies. To achieve this, several promoter-reporter vectors can be used for *in vivo* transfection where the expression of the enzyme is driven by constitutive eukaryotic promoters/enhancers (i.e. HZCX-HSV-*lacZ* amplicon vector or pCMV-*β*-Gal). In this case, mice are xenografted and then treated with some of those vectors. A second approach consists of the transfection of cells *in vitro* which are later injected in mice. Probes **73**-**79** in Chart **5** were designed to detect *β*-Gal activity *in vivo* induced by *lacZ* gene.

Apart of these approaches for the detection of *β*-Gal activity *in vivo*, some examples include the use of mice models with cell lines which endogenously overexpressed *β*-Gal (probes **80**-**82** in Chart **6**) and tracking of *β*-Gal activity by senescence-inducing chemotherapy (probes **83** to **86** in Chart **7**).

Chart 5. Structure of probes **71**-**79**.

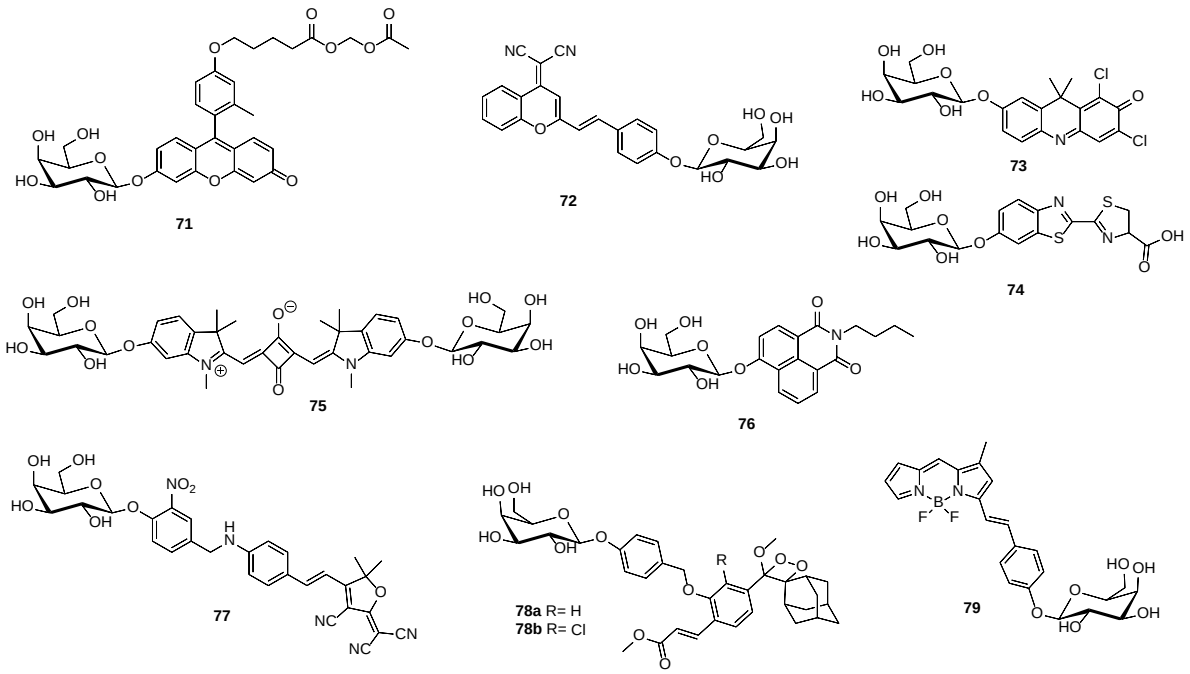

Probe **71** was synthesized by Urano and co-workers and was successfully employed to visualize *β*-Gal activity *in vivo* and *ex vivo*.[88] **71** contains a *β*-galactosyl moiety and two ester linkages yielding, after its hydrolysis with *β*-Gal and esterases, a hydrophilic carboxylate derivative that was expected to be retained by cells. PBS (pH 9.0) solutions of **71** presented very weak emission at 518 nm upon excitation at 453 nm. In the presence of *β*-Gal enzyme, **71** was converted to the highly fluorescent compound **71a** with a 470-fold emission enhancement (Scheme **6a**). Confocal microscopy studies, carried out with HEK293 cells expressing *β*-Gal incubated with **71**, showed a marked green fluorescence indicative of an efficient internalization and enzymatic-induced hydrolysis of the probe yielding the highly emissive dye **71b** (Scheme **6a**). Mice xenografted with SHIN3 ovarian cancer cells were used to test **71** *in vivo*. In a first step, avidin-*β*-Gal (selected due to its high affinity for lectins on the surface of SHIN3 cells) was injected intraperitoneally into mice bearing SHIN3 tumors. To these SHIN3 xenografted mice, probe **71** was intraperitoneally administered and incubated for 1 h. After the incubation period a strong emission in the peritoneal cavity, mainly located in small tumors in the mesenterium, was observed and was ascribed to *in vivo β*-Gal hydrolysis of **71**. Besides, almost no fluorescence was observed in normal tumour-free mice treated with **71**.

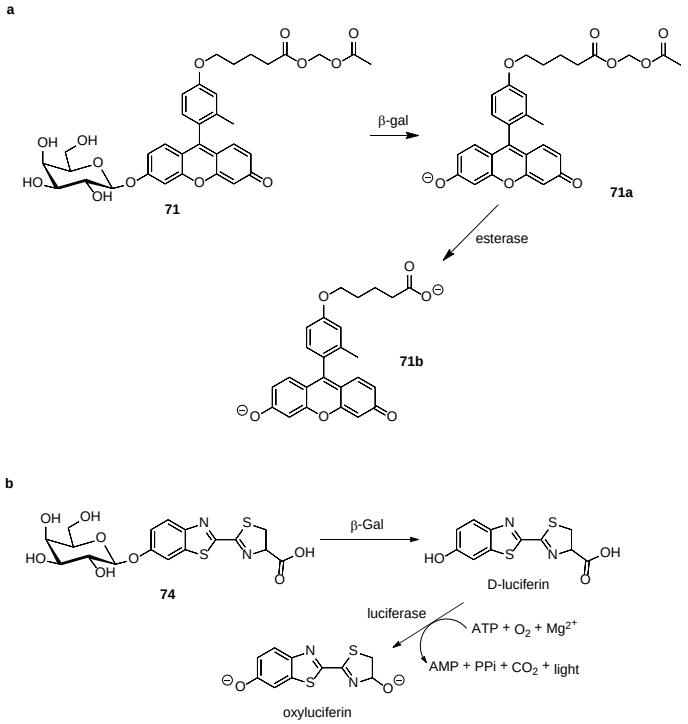

Scheme 6. Hydrolysis mechanism of (a) probe **71** and (b) probe **74**.

Zhu and co-workers synthesized a *β*-Gal targeting ratiometric NIR fluorescent probe in which the dicyanomethylene-4*H*-pyran chromophore was linked to a galactose group (**72**).[89] The authors showed that upon excitation at 535 nm, a remarkable NIR emission at 685 nm was found due to the dicyanomethylene-4H-pyran fluorophore generate after *β*-Gal hydrolysis of the glycosidic bond. Probe **72** was tested in human embryonic kidney 293T cells transfected by *lacZ* gene to overexpress *β*-Gal. In control 293T cells, where **72** was not hydrolyzed, the fluorescent signal was observed in the green channel (from 490 to 530 nm) when excited at 404 nm, whereas in *lacZ* positive cells, **72** was detected in the red channel (from 650 to 720 nm) when exciting at the same wavelength. Moreover, upon excitation at 560 nm, *lacZ* positive cells showed a clear fluorescent signal in the NIR region (from 605 to 725 nm). **72** was also tested with OVCAR-3 cells, from human ovarian cancer patients (with endogenous *β*-Gal), and the authors obtained similar results to those found with 293T-*lacZ* positive cells. Furthermore, the fluorescence signal was not observed after treating 293T-*lacZ* positive cells with D-galactose, an inhibitor of *β*-Gal. *In vivo* studies were carried out by using LoVo cell xenografts in mice. Tumors were transfected with avidin-*β*-Gal. Then, **72** was intratumorally injected in control mice and mice treated with avidin-*β*-Gal, and studied by IVIS. Fluorescent images were only observed in labeled tumors with avidin-*β*-Gal.

Weissleder and co-workers used 9H-(1,3-dichloro-9,9-dimethylacridin-2-one-7-yl) *β*-D-galactopyranoside (**73**) as a far-red fluorogenic probe which suffers a dramatic bathochromic shift when hydrolyzed by *β*-Gal, yielding 9H-(1,3-dichloro-9,9- dimethylacridin-2-one-7-yl).[90] **73** was tested in 9L gliosarcoma cells and 9L-*lacZ* transfected cells. Using excitation wavelengths higher than 600 nm only the hydrolytic product was excited but no the **73** precursors, so that, 9L-*lacZ* cells treated with **73** showed considerable higher fluorescence than 9L control cells. In addition, 9L and 9L-*lacZ* xenografts were co-implanted in nude mice's chest and treated with **73**. It was observed a 4-fold higher fluorescent signal in 9L-*lacZ* tumors compared with 9L control tumors. Moreover, the authors tested the method by infecting human glioma Gli36 tumor cells through a viral vector (HZCX-HSV amplicon vector containing the *lacZ* gene) and demonstrated that amplicon-infected cells were also able to hydrolyze **73**. Finally, mice bearing Gli36 and Gli36-*lacZ* xenografts were treated with **73**. It was found a 3-fold higher fluorescence signal in Gli36-*lacZ* compared with non-infected Gli36 tumors.

Blau and co-workers developed a sequential reporter-enzyme luminescence assay for the *in vivo* detection of *β*-Gal activity.[91] The D-luciferin-galactoside conjugate **74** was non-emissive, however, in the presence of *β*-Gal enzyme, **74** is hydrolyzed to galactose and D-luciferin and the later, in the presence

of ATP and luciferase, yielded oxyluciferin and light (Scheme **6b**). The sensing ability of the prepared probe was tested using C2C12 myoblasts engineered to overexpress luciferin alone or luciferin with *β*-Gal (using *lacZ*). The C2C12 cells overexpressing luciferase did not show any luminescence after the treatment with probe **74**. On the contrary, C2C12 cells that overexpress luciferase and *β*-Gal showed marked luminescence after **74** internalization. Besides, C2C12 cells with overexpressed luciferase were injected in the left tibialis anterior muscle of BALB/c nude mice, and the same cells overexpressing luciferin and *β*-Gal in the right tibialis anterior muscle. The *in vivo* luminescence profile obtained, after intraperitoneal injection of **74**, showed a 30 to 200-fold greater signal in the right than in the left leg. The probe was also successfully used to detect *β*-Gal activity in transgenic mice.

Nagano and co-workers synthesized the squarylium derivative bearing two *β*-galactosyl moieties **75** for the visualization of *β*-Gal activity both *in vitro* and *in vivo*.[92] PBS solutions (pH 7.4 containing 1% w/v of BSA) of **75** showed a weak fluorescence at 652 nm. Upon addition of *β*-Gal enzyme, the emission band was redshifted to 660 nm and its intensity was moderately enhanced due to the *β*-Gal-induced hydrolysis of the *β*-galactosyl moieties yielding the corresponding squarylium dye. Probe **75** was successfully used to detect *β*-Gal activity in HEK293 cells transfected with a plasmid encoding *lacZ* gene. Besides, the ability of **75** to detect *β*-Gal activity *in vivo* was assessed using ICR mice injected with a *β*-Gal-encoding plasmid (pCMV-*lacZ*) targeting the liver. Then, **75** was intravenously injected in mice and fluorescent images were acquired sequentially for 30 min. The images showed a progressive fluorescence intensity increase in the liver demonstrating the ability of the probe to detect *β*-Gal activity *in vivo*.

Han et al. prepared the naphtalimide-*O*-galactose two-photon probe **76** for the detection of *E. coli β*-Gal in cells and *in vivo*.[93] PBS solutions of **76** presented an intense emission at 440 nm (excitation at 395 nm) and the addition of *β*-Gal induced a marked quenching of this band together with the appearance of a weak fluorescence at 545 nm. *In vitro* studies were carried out with C6 cells as control and C6 transfected with *lacZ* to overexpress *β*-Gal. The authors observed a fluorescent signal in the blue channel (410-460 nm) after treatment C6 control cells with **76**, whereas, for *lacZ* positive C6 cells, the fluorescent images were observed in the yellow channel (520-570 nm), due to the hydrolysis of the probe. For *in vivo* studies, xenografts of U-87 MG were established in nude mice. Tumors were transfected with pCMV-*lacZ* plasmid to overexpress *β*-Gal. Then, **76** was intratumouraly injected and a fluorescent signal in transfected tumors (10-fold higher in comparison with non-transfected tumors) was observed.

Kim et al. synthesized a NIR ratiometric fluorescent probe (**77**) for *in vivo* detection of *β*-Gal in hepatocyte HepG2 cells and its corresponding xenograft model.[94] The probe consisted of a galactose moiety as a triggering site, a self immolative linker, and a dicyanomethylenedihydrofuran fluorophore. **77** was able to target hepatocyte cells, which have the ASGPR receptor overexpressed, and mediated *β*-Gal-specific activation. **77** showed a marked emission at 615 nm when excited at 580 nm, whereas in presence of *β*-Gal the emission band shifted to 665 nm because of the hydrolysis of the glycosidic bond. The authors confirmed the cellular uptake of **77** in HepG2 cells (ASGPR positive) by confocal microscopy and flow cytometry, whereas the fluorescence signal was not detected in A549 and KB cells (both ASGPR negative). The preferential uptake of **77** in HepG2 cells was ascribed to the presence in the probe of galactose, which is an efficient ligand of the ASGPR receptor. The ratiometric profile of **77** in presence of *β*-Gal was also studied in HepG2 cells treated with pCMV-*lacZ* to overexpress *β*-Gal (HepG2-*lacZ*). No transfected HepG2 cells were used as control. Approximately a 2.1-fold fluorescence enhancement was observed in the case of HepG2-*lacZ* transfected cells when treated with **77**. HepG2 and HepG2-*lacZ* xenograft were established subcutaneously in both flanks of mice. Mice were studied under whole-body *in vivo* fluorescence imaging. As **77** has galactose as an efficient targeting ligand for ASGPR on HepG2 tumor, obvious fluorescence signals were detected in both tumors with higher intensity in the case of *lacZ* positive tumor. Besides, *ex vivo* imaging studies by confocal microscopy also revealed that fluorescence was significantly higher in HepG2-*lacZ* transfected xenograft.

Chemiluminescent compounds normally emit light through oxidation mechanisms. Only phenoxy-dioxetanes, introduced by Schaap in 1987, are known to trigger chemiluminescence through another reaction than oxidation.[95] Scheme **7** shows the typical chemically/enzymatically activation mechanism of phenoxy-dioxetanes which are stable high-energy oxidized species at room temperature, yet when the phenol is deprotected, light emission is activated.

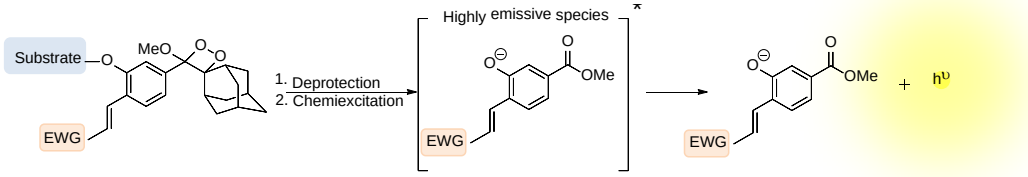

Scheme 7. Activation pathway of dioxetane probes.

Quantum yields of phenoxy-dioxetanes are high in organic solvents, but decrease about 10,000 times in aqueous solution. The problem of the low emission of dioxoethanes in aqueous solvents has recently been solved by Shabat et al. who introduced an ortho acrylate substituent respect to the phenolic group and a chlorine substituent at the flanked position to the phenol moiety (**78b**). The introduction of a chlorine atom in the flanked position reduces pK_a of phenol allowing the chemiexcitation process to occur at physiological pH. Probe **78b** is composed of chlorine-acrilate-phenoxy-dioxetanes luminophore linked to a *β*-galactopiranoside moiety through an *O*-phenolic linkage. Moreover, **78a** is the same probe without the chlorine group.[96] In order to compare **78b** vs. **78a**, control, and *lacZ*-transfected CT26 colon cancer cells were incubated with both probes, observing that signal in *lacZ(+)*CT26 was around 10-fold higher for **78b** than **78a**, while *lacZ(-)*CT26 showed a negligible signal. Finally, the solubility of **78b** and **78a** was enhanced by conjugating them with CGKRK peptide for *in vivo* experiments. Probe **78b** was intratumorally injected in control or *lac*Z-transfected CT26 tumor-bearing BALB/c mice, observing a 20-fold higher luminescent signal for *lacZ(+)*CT26 tumor-bearing animals compared to control ones. However probe **78a** did not produce any luminescent signal in either *lacZ(+)* nor *lacZ(+)*CT26 tumor-bearing mice, probably due to its reduced photostability ascribed to the higher pK_a of the phenolic group.

In 2019, Zhu and co-workers prepared **79** (based on a BODIPY fluorophore linked with a galactose unit), a ratiometric probe for the detection of *β*-Gal enzyme directly injected in tumors *in vivo*.[97] PBS/DMSO solutions of **79** showed a marked emission band at 575 nm that was progressively quenched in the presence of *β*-Gal. Besides a new fluorescence appeared at 730 nm which was ascribed to the deprotonated BODIPY fluorophore. The ratiometric fluorescent ratio (I_{730}/I_{575}) showed a linear dependence of *β*-Gal concentration and a LOD of 4.6 x 10^{-3} U mL^{-1}. SKOV-3 cells (endogenous *β*-Gal) incubated with **79** showed a weak fluorescence signal in the green channel (570-620 nm) and a strong fluorescence in the red channel (670-800 nm) indicating the presence of *β*-Gal. On the other hand, only fluorescence in the green channel was observed for HepG2 cells (negative control) treated with **79**. Besides, **79** was used for the real-time *in vivo* visualization of *β*-Gal activity in tumors. The authors used human lung xenograft tumor cells (A549 cells) that not overexpressed *β*-Gal. Mice tumors were injected with *β*-Gal and then **79** was injected orthotopically. Negative control was injected with PBS and then with **79**. Negative control only showed strong fluorescence emission in the green channel. However, pre-treated *β*-Gal tumor-bearing mouse exhibits a strong fluorescence signal at 763 nm after 5 min post-injection.

Apart from the examples described above, probes **80**-**82** in Chart **6** were designed to tracking *β*-Gal activity in tumors that presented high levels of enzymatic activity. These tumors contain cell lines that endogenously overexpressed *β*-Gal such as SHIN3, SKOV3, OVK18, OVCAR3, OVCAR4, OVCAR5, OVCAR8, or HUVEC.

Chart 6. Structure of probes **80**, **81** and **82.**

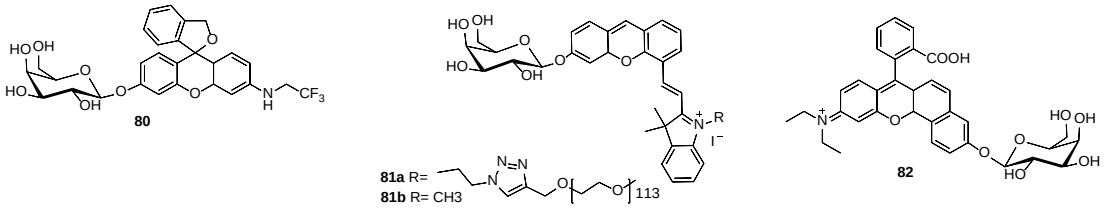

Urano et al. synthesized probe **80**, based on a hydroxymethyl rhodol fluorophore linked with galactose, and tested its ability to detect *β*-Gal in seven human peritoneal ovarian cancer cell lines (SHIN3, SKOV3, OVK18, OVCAR3, OVCAR4, OVCAR5, OVCAR8 or HUVEC) which overexpress this enzyme at different levels.[98] The authors validated the probe by confocal microscopy in these cells lines. In all cases, an emission in the 505–600 nm range was found when excited at 498 nm. Moreover, the signal decreased when the cells were treated with *β*-galactosylamidine, an inhibitor of *β*-Gal. Moreover, a model of peritoneal metastasis mice, using SHIN3, SKOV3, OVK18, OVCAR3, OVCAR4, OVCAR5, OVCAR8, or HUVEC cells were treated with the probe, and tumors were detected by fluorescence spectral imaging. The author also made *in vivo* fluorescence endoscopy for the detection of metastases. In this case, **80** was intraperitoneally administrated and the product of the hydrolysis detected by fluorescence laparoscopy.

Probes **81a** and **81b** are formed by a NIR hemicyanine fluorophore (with a hydrophilic PEG chain in **81a** and a methyl group in **81b**) linked with a galactose unit.[99] Both probes were non-emissive but marked emission bands at 720 and 712 nm for **81a** and **81b** were observed after incubation with *β*-Gal. Besides, the fluorophores obtained after *β*-Gal hydrolysis presented absorption bands at 680 nm. Both probes presented photo-thermal features. At this respect, under laser irradiation (680 nm) of solutions of probes **81a** and **81b** in the presence of *β*-gal enzyme, a remarkable enhancement of temperature was observed after 180 s (reaching 48 and 37ºC for **81a** and **81b** respectively). *In vitro* studies showed a marked NIR emission in SKOV3 cells (which overexpressed *β*-Gal) after internalization of both probes whereas negligible fluorescence was observed in NIH-3T3 (negative control). The authors evaluated probes in subcutaneous a SKOV3 xenograft tumor model. Finally, the photo-thermal effect was studied in SKOV3tumor-bearing mice after 1 h post-injection of both probes irradiated for 5 min with a 680 nm laser. The maximal tumor temperature of **81a**-treated mice was 48.3 ºC, which was 9.5 and 9.3 ºC higher than those obtained for **81b** and saline-treated mice. These data allowed the cellular ablation (43 ºC) employing **83a** with the successful suppression of tumor growth. However, **81b** did not show therapeutic effect.

Recently, a two-photon probe **82**, based on a rhodamine derivative linked with a galactose unit through an *O*-glycosidic bond, for *β*-Gal detection was described.[100] PBS solutions of **82** showed a broad emission band at 590 nm (excitation at 550 nm) that was progressively vanished in the presence of *β*-Gal. At the same time, a new emission at 638 appeared, which was ascribed to the deprotonated fluorophore. From the titration profile, a limit of detection of 4.13×10^{-4} U·mL^{-1} for *β*-Gal was measured. OVCAR-3 cells (with endogenous *β*-Gal) incubated with **82** showed strong fluorescence in the red channel whereas negligible emission was observed for HeLa cells (control) treated with the probe. *In vivo* experiments were carried out in mice subcutaneously xenografted with OVCAR-3 or HeLa tumors cells and then treated with **82**. OVCAR-3 tumors showed high fluorescent intensity in comparison with that observed with HeLa due to the overexpression of *β*-Gal in the former. Besides, **82** was successfully used for *ex vivo* imaging of OVCAR-3 tumor tissues employing two-photon microscopy.

Senescence, and its associated *β*-Gal activity, can be induced by chemotherapy *in vivo*. Current research suggests that chemotherapy-induced senescence represents a novel functional target that may improve therapy against cancer and aging-related diseases.[52, 101, 102] Recently several probes for detection of *β*-Gal activity induced by chemotherapy *in vivo* were recently published (probes **83** to **86** in Chart **7**).

Chart 7. Structures of probes **83**-**86**.

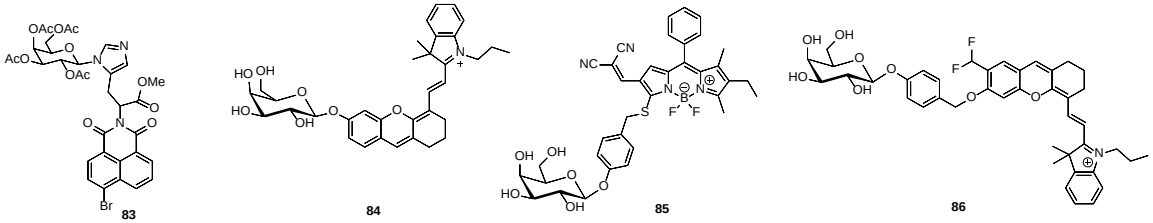

This approach was used by Martínez-Máñez and co-workers who designed a naphthalimide-based two-photon probe containing an L-histidine methyl ester linker and an acetylated galactose attached to one of the aromatic nitrogen atoms of the L-histidine for the detection of cell senescence (**83**).[103] Solutions of **83** did not show any significant fluorescence when exciting at 405 nm, however, when *N*-glycosidic bond was hydrolyzed an intense band centred at 540 nm appeared. Targeting of senescent cells *in vitro* with **83** was validated with SK-MEL-103 (human melanoma) cell line as a control, and the same SK-MEL-103 treated with palbociclib for two weeks in order to induce senescence. Cells were then analyzed by two-photon confocal microscopy using 750 nm as the excitation wavelength, observing not noticeable fluorescence signal in control cells treated with **83**. In contrast, senescent cells incubated with **83** displayed a clear bright emission attributed to the hydrolysis of *N*-glycosidic bond that selectively occurred in senescent cells. The probe was also tested in mice bearing tumor xenografts of SK-MEL-103 cells. Mice were treated with palbociclib for 10 days to induce senescence. Then, both control and senescent tumor-bearing mice were treated intravenously with **83** and sacrificed after 3 h. Control tumors showed negligible fluorescence either in the absence or in the presence of **83**. In sharp contrast, tumors from mice treated with palbociclib and intravenously injected with **83** showed a strong fluorescent signal. Moreover, the same authors reported a selective-delivery carrier that was able to release its cargo in senescent cells. The nanodevice consisted of mesoporous silica nanoparticles (MSNs), loaded with rhodamine B, functionalized with 3-aminopropyltrialcoxisilane (APTES), and capped with a galacto-oligosaccharide (GOS).[23] A poor cargo release was observed for the capped nanoparticles, whereas in presence of the enzyme a remarkable amount of rhodamine B was released after 24 h due to the hydrolysis of the capping galacto-oligosaccharide (Scheme **8a**). The nanoparticles were tested in the cells lines DC1787, X-DC 1774, and X-DC4646 from patients suffering dyskeratosis congenita, in which *β*-Gal is overexpressed. High emission signals were found in DC1787, X-DC 1774, and X-DC4646 cell lines, whereas no cargo delivery was found in H460 control cells where *β*-Gal is not overexpressed. More recently, the same authors reported MSNs loaded with the NIR-FDA approved Nile blue (NB) and capped with a galactohexasaccharide (GalNP(NB)). NB is stacked inside the pores and its emission at 672 nm is highly quenched, yielding a strong fluorescent signal after cap hydrolysis in the presence of *β*-Gal and dye release.[104] The quenching effect inside the MSNs pores was demonstrated by comparing fluorescence spectrums of NB solution (highly emissive) and GalNP(NB) suspension (non-emissive) at equivalent concentrations of the dye and by plotting the emission intensity of NB solutions vs. fluorophore concentration, showing that NB concentrations higher than 10^{-3} M were poorly emissive. Specific targeting of senescent cells *in vitro* with GalNP(NB) was demonstrated in SK-Mel-103 (human melanoma) and 4T1 (murine breast cancer) cells treated with the senescence inducer palbociclib. When both cell lines were incubated with GalNP(NB), confocal studies revealed a clear bright fluorescence emission only in senescent cells, while both cell lines incubated with the free NB fluorophore, showed high fluorescent signal in control and in senescent cells, which demonstrated the selectivity of GalNP(NB). Moreover, the probe was able to detect cellular senescence *in vivo* in palbociclib-treated BALB/cByJ mice bearing breast cancer tumors, observing an increase in fluorescence intensity up to 24 h post-injection and a subsequent decrease and disappearance after 48 h post-injection. Finally, blood biochemistry and hematology analysis showed no signs of organ damage and systemic inflammatory response after MSNs administration. Besides, biodistribution studies revealed that nanoparticles reach both senescent and non-senescent tumors at 24 h, whereas levels of Si are significantly reduced 48 h post-injection, which was consistent with the patterns of fluorescence signal.

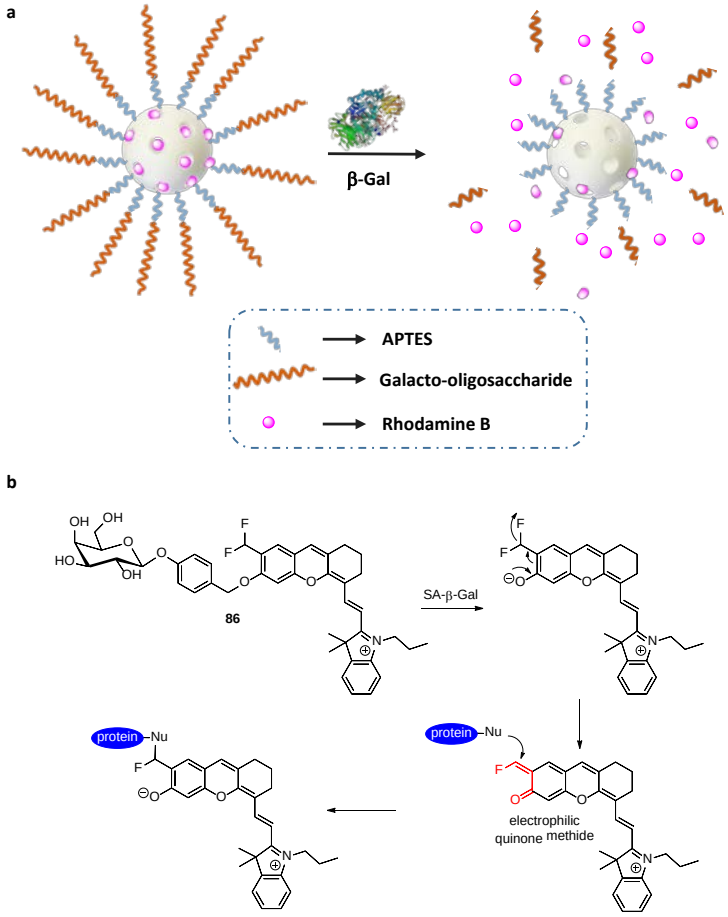

Scheme 8. (a) Mesoporous silica nanoparticles capped with a galacto-oligosaccharide. In the presence of *β*-Gal the galacto-oligosaccharide cap is hydrolysed and cargo is released. (b) Hydrolysis mechanism of probe **86**.

In 2019 Cui and co-workers described probe **84**, which consisted in a hemicyanine fluorophore linked with a galactose unit.[105] Aqueous solutions of **84** were nearly non-emissive, whereas in the presence of *β*-Gal a marked fluorescence at 708 nm (excitation at 680 nm) was observed ascribed to the enzyme-induced hydrolysis of the glycosidic bond with subsequent hemicyanine release. The limit of detection obtained was 0.0031 unit·mL^{-1} (0.13 nM). *In vitro* test were carried out using CT26.CL25, a mouse colon fibroblast carcinoma cell line that expresses *β*-Gal due to the transfection of *LacZ* gene, and CT26-WT cells. Flow cytometry studies, carried out with both cell lines treated with **84**, showed a marked fluorescence in CT26.CL25 whereas only background signal was detected in CT26.WT. Besides, the authors incubated HeLa and MCF7 senescent cells (induced with camptothecin) with **84** and observed a marked fluorescence as a consequence of probe hydrolysis by *β*-Gal overexpressed in these cells. The authors used two different approaches for the detection of *β*-Gal *in vivo*. In a first experiment used the genetically modified mice colon cancer CT26 cell line to determine whether **84** could differentiate tumors with and without active *β*-Gal. Tumors with the *LacZ(+)* CT26.CL25 cells showed higher fluorescent signal that tumour with CT26WT cells. These results suggest the activation of **84** in the presence of *β*-Gal expressed cells. In a second experiment, **84** was tested in HeLa xenograft mice models to corroborate the capacity of the probe to detect the overexpressed *β*-Gal in camptothecin-induced senescence tumors. Probe **84** was injected two days after camptothecin treatment resulting in a marked fluorescence in the tumors.

Gu and co-workers prepared probe **85** and tested its ability for *in vivo* imaging of senescent vascular cells.[106] PBS-DMSO 7:3 v/v solutions of probe **85** showed an emission band centred at 580 nm (excitation at 488 nm) that was quenched in the presence of *β*-Gal enzyme. Besides, a new emission band at 730 nm appeared indicating that probe **85** could be used as a ratiometric sensor. From the titration

profile obtained with the addition of increasing amounts of *β*-Gal enzyme, a limit of detection of 0.014 U mL^{-1} was obtained. The observed results were ascribed to the enzymatic hydrolysis of the glycosidic bond, elimination of the linker and generation of a highly emissive BODIPY fluorophore. VSMCs senescent cells (in which senescence is induced with Ang II) showed a marked red fluorescence and a very small emission in the green zone with a fluorescence ratio I_{red}/I_{green} of 4.8. As a clear contrast, I_{red}/I_{green} ratio for normal VSMCs cells was only 0.4. For the *in vivo* studies, probe **85** was encapsulated in poly(lactic-*co*-glycolic) acid nanoparticles. $ApoE^{-/-}$ mice pretreated with Ang II were used as a model of atherosclerosis (atherosclerotic vascular cells presented features of cellular senescence). Injection of nanoparticles via the caudal vein of the mice pretreated with Ang II showed a marked emission when compared to control animals (without Ang II administration). Besides, a marked fluorescence signal was observed in the aortic arch of the atherosclerotic mice. Finally, Cui and co-workers developed the self-immobilizing NIR probe **86** for the imaging of senescent cells.[107] PBS solutions of probe **86** are nearly non-emissive (excitation at 675 nm) whereas in the presence of *β*-Gal enzyme a new fluorescence at 708 nm appeared (16-fold enhancement). Confocal microscopy studies showed a marked emission in the red channel for senescent HeLa cells (senescence induced with camptothecin) and for CT26.CL25 cells (overexpressed *β*-Gal) administered with probe **86**, whereas negligible fluorescence was observed for normal HeLa and CT26.WT cells. *In vivo* studies were carried out with mice bearing HeLa tumors treated with camptothecin and administered with probe **86**. IVIS images showed a marked fluorescence in the mice treated with camptothecin and **86** whereas negligible signals were observed in mice only treated with the probe alone. Besides, the emission signal remained more than 24 h due to the attachment of the *in situ* generated fluorophore to proteins (see Scheme **8b**).

5. Conclusions and Future Perspectives

The detection and control of enzyme levels is an analytical technique for corroborate the health of patients and can be used as a tool in the detection of different diseases. In the present review, we have detailed different probes that are used for *β*-Gal enzyme detection *in vitro* and *in vivo*. The first chromo-fluorogenic molecular probes described were able to detect *β*-Gal activity in solution and *in vitro* using different cell lines transfected with *lacZ* gene to induce the overexpression of this enzyme. Moreover, in the last years, molecular probes for monitoring and detection of *β*-Gal activity *in vivo* animal models have been described. In spite of these promising examples, some of the described probes still present some drawbacks such as unsuitable excitation and emission wavelengths, poor cellular membrane permeability, absence of data about their potential application in more realistic cellular or animal models, and reduced chemical stability. The use of two-photon fluorophores in the design of these probes has been still poorly studied and can ameliorate some of these drawbacks. These fluorophores allowed excitation with long-wavelength light (more penetrating and safer for tissues) and it can be envisioned that a next generation of fluorogenic molecular probes for the detection of *β*-Gal activity using two-photon or NIR fluorophores with marked sensitivities and more suitable for *in vivo* tracking applications will be described in the near future. Besides, most probes reported by now are based on the linking, through *O*- or *N*-glycosidic linkages, of selected fluorophores with D-galactose as recognition subunit. The use of nanoparticles for the controlled release of fluorophores [108,109,110] in cells overexpressing *β*-Gal enzyme is also a promising strategy for their detection but still not fully developed. These hybrid nanodevices would not only sense *β*-Gal but also selectively deliver their cargo in cells which overexpressed *β*-Gal additionally reducing unwanted harmful side effects of the loaded molecules.[111] Finally, we hope this review to not only help researchers who work in the field of enzyme detection but also may open the minds of related ones to develop new advances in this fertile research area.

6. Acknowledgments

R.M laboratory members thank the financial support from the Spanish Government (project RTI2018-100910-B-C41) and the Generalitat Valenciana (project PROMETEO 2018/024). B.L-T. is grateful to the

Spanish Ministry of Economy for their PhD grants (FPU15/02707). J. F.-B thanks to his postdoctoral fellowship (CD19/00038).

7. Compliance with ethical standards

Conflicts of interest. The authors declare that they have no conflict of interest.

8. References

1 Fernandes, P. Enzymes in food processing: a condensed overview on strategies for better biocatalysts. Enzyme Res. 2010;2010:86253-73.
2 Likidlilid A, Patchanans N, Peerapatdit T, Sriratanasathavorn C. Lipid peroxidation and antioxidant enzyme activities in erythrocytes of type 2 diabetic patients. J Med Assoc Thai. 2010;93(6):682-93.
3 Pinto N, Dolan ME. Clinically relevant genetic variations in drug metabolizing enzymes. Curr Drug Metab. 2011;12(5):487-97.
4 Giannini EG, Testa R, Savarinom V. Liver enzyme alteration: a guide for clinicians. CMAJ. 2005;172(3):367-79.
5 Peters C, Shapiro EG, Krivit W. Hurler syndrome: Past, present, and future. J. Pediatr. 1998;133(1):7-9.
6 Rodriguez M, O'Brien JS, Garrett RS, Powell HC, Canine GM1 gangliosidosis: An ultrastructural and biochemical study. J. Neuropathol. Exp. Neurol. 1982;41(6):618-29.
7 Cozma C, Eichler S, Wittmann G, Flores Bonet A, Kramp G, Giese AK, Rolfs A. Diagnosis of Morquio syndrome in dried blood spots based on a new MRM-MS assay. PLoS One. 2015;10(7):e0131228.
8 Suzuki K, Suzuki Y. Globoid cell leucodystrophy (Krabbe's disease): deficiency of galactocerebroside beta-galactosidase. Proc Natl Acad Sci U S A. 1970;66(2):302-9.
9 Holtzman D, Ulrich J. Senescent glia spell trouble in Alzheimer's disease. Nat. Neurosci. 2019;22(5):683–84.
10 Robert L, Fulop T. Aging: Facts and theories. Indian J Med Res. 2016;143(3):385-86.
11 Dimri GP, Lee X, Basile G, Acosta M, Scott G, Roskelley C, et al. A biomarker that identifies senescent human cells in culture and in aging skin *in vivo*. Proc. Natl Acad. Sci. USA. 1995;92(20):9363–7.
12 Biran A, Zada L, Karam PA, Vadai E, Roitman L, et al. Quantitative identification of senescent cells in aging and disease. Aging Cell. 2017;16(4):661-71.
13 (a) Grynkiewicz G, Poenie M, Tsien RY. Grynkiewicz G, Poenie M & Tsien RY. A new generation of Ca^{2+} indicators with greatly fluorescence properties. J Biol Chem. 1985;260(6):3440-50; (b) de Silva AP, Gunaratne HQN, Gunnlaugsson T, Huxley AJ, McCoy CP, Rademacher JT, Rice TE, Signaling recognition events with fluorescent sensors and switches. Chem. Rev. 1997;97(5):1515-66; (c) Que EL, Domaille DW, Chang CJ. Metals in neurobiology: probing their chemistry and biology with molecular imaging. Chem. Rev. 2008;108(5):1517-49; (d) Ueno T, Nagano T. Fluorescent probes for sensing and imaging. Nat. Methods. 2011;8(8):642-5; (e) Kobayashi H, Ogawa M, Alford R, Choyke PL, Urano Y. New strategies for fluorescent probe design in medical diagnostic imaging. Chem. Rev. 2010;110(5):2620-40; (f) Valeur B, Leray I. Design principles of fluorescent molecular sensors for cation recognition. Coord. Chem. Rev. 2000;205(1):3-40.
14 Kim HM, Cho BR. Small-Molecule Two-Photon probes for bioimaging applications. Chem. Rev. 2015;115(11):5014-55.
15 (a) Huang J, Pu K. Activatable molecular probes for second near-infrared fluorescence, chemiluminescence, and photoacoustic imaging. Angew. Chem. Int. Ed. 2020;59(29):11717-31; (b) Miao Q, Pu K. Organic semiconducting agents for deep-tissue molecular imaging: Second Near-Infrared fluorescence, self-luminescence, and photoacoustics. Adv Mater. 2018;30(49):e1801778.
16 Cheng P, Miao Q, Li J, Huang J, Xie C, Pu K. Unimolecular chemo-fluoro-luminescent reporter for crosstalk-free duplex imaging of hepatotoxicity. J. Am. Chem. Soc. 2019;141(27):10581-84.
17 (a) Wei H, Wu G, Tian X, Liu Z. Smart fluorescent probes for in situ imaging of enzyme activity: design strategies and applications. Future Med. Chem. 2018;10(23):2729-44; (b) Liu HW, Chen L, Xu C, Li Z, Zhang H, Zhang XB, Tan W. Recent progresses in small-molecule enzymatic fluorescent probes for cancer imaging. Chem. Soc. Rev. 2018;47(18):7140-80.
18 Huang J, Li J, Lyu Y, Miao Q, Pu K. Molecular optical imaging probes for early diagnosis of drug-induced acute kidney injury. Nat. Mater. 2019;18, 1133-43.
19 Roth ME, Green O, Gnaim S, Shabat D. Dendritic, oligomeric, and polymeric self-immolative molecular amplification. Chem. Rev. 2016;116(3):1309-52.

20 Zhang J, Cheng P, Pu K. Recent advances of molecular optical probes in imaging of β-Galactosidase. Bioconjugate Chem. 2019;30(8):2089-101.
21 Lozano-Torres B, Estepa-Fernández A, Rovira M, Orzáez M, Serrano M, Martínez-Máñez R, Sancenón F. The chemistry of senescence. Nat. Rev. Chem. 2019;3:426-41.
22 Mazur A, Kro´l JE, Marczak M, Skorupska A. Membrane Topology of PssT, the transmembrane protein component of the Type I exopolysaccharide transport system in Rhizobium leguminosarum bv trifolii Strain TA1. J Bacteriol. 2003;85(8):2503-11.
23 Agostini A, Mondragón L, Bernardos A, Martínez-Máñez R, Marcos MD, Sancenón F. et al. Targeted cargo delivery in senescent cells using capped mesoporous silica nanoparticles. Angew. Chem. Int. Ed. 2012;51(42):10556-60.
24 Asanuma D, Sakabe M, Kamiya M, Yamamoto K, Hiratake J, Ogawa M. et al. Sensitive β-galactosidase-targeting fluorescence probe for visualizing small peritoneal metastatic tumours *in vivo*. Nat Commun;2015(6):6463.
25 (a) Rotman B. Measurement of activity of single molecules of β-D-Galactosidase. Proc. Natl. Acad. Sci. USA. 1961;47(12):1981-91; (b) Rotman B, Zderic JA, Edelstein M. Fluorogenic substrates for beta-D-galactosidases and phosphatases derived from flurescein (3,6-dihydroxyfluoran) and its monomethylether. Proc. Natl. Acad. Sci. USA. 1963;50(1):1-6.
26 Mandal PK, Cattiaux L, Bensimon D, Mallet J.M. Monogalactopyranosides of fluorescein and fluorescein methyl ester: synthesis, enzymatic hydrolysis by biotnylated β-galactosidase, and determination of translational diffusion coefficient. Carbohydr. Res. 2012;358(40):40-6.
27 Stracean R, Wooda J, Irschmann R. Synthesis and Properties of 4-Methyl-2-oxo-1,2-benzopyran-7-yl β-D-Galactoside (Galactoside of 4-Methylumbelliferone). J. Org. Chem. 1962;27(3):1074-75.
28 Gee KR, Sun WC, Bhalgat KM, Upson RH, Klaubert DH, Latham KA. et al. Fluorogenic substrates based on fluorinated umbelliferones for continuous assays of phosphatases and beta-galactosidases. Anal. Biochem. 1999;273(1):41-8.
29 Chilvers KF, Perry JD, James AL, Reed RH. Synthesis and evaluation of novel fluorogenic substrates for the detection of bacterial beta-galactosidase. J. Appl. Microbiol. 2001;91(6):1118-30.
30 Aizawa K. Studien über Carbohydrasen, I. I. Die fermentative Hydrolyse des p-nitrophenol-β-galactoside. Enzymologia.1939;6:321-24.
31 Na SY, Kim HJ. Fused oxazolidine-based dual optical probe for galactosidase with a dramatic chromogenic and fluorescence turn-on effect. Dyes Pigments. 2016;134:526-530.
32 Corey PE, Trimmer RW, Biddlecom WG. A new chromogenic β-Galactosidase substrate: 7-β-D-Galactopyranosyloxy-9,9-dimethyl-9H-acridin-2-one. Angew. Chem. Int. Ed. 1991;30(12):1646-48.
33 Wang P, Du J, Liu H, Bi G, Zhang G. Small Quinolinium-Based enzymatic probes via blue-to-red ratiometric fluorescence. Analyst. 2016;141:1483-7.
34 Otsubo T, Minami A, Fujii H, Taguchi R, Takahashi T, Suzuki T, Teraoka F, Ikeda K. 2-(Benzothiazol-2-yl)-phenyl-β-d-galactopyranoside derivatives as fluorescent pigment dyeing substrates and their application for the assay of β-d-galactosidase activities. Bioorg. Med. Chem. Lett. 2013;23(7):2245-9.
35 Sun C, Zhang X, Tanga M, Liu L, Shi L, Gao C. et al. New optical method for the determination of β-galactosidase and α-fetoprotein based on oxidase-like activity of fluorescein. Talanta;194:164-70.
36 Hirabayashi K, Hanaoka K, Takayanagi T, Toki Y, Egawa T, Kamiya M. et al. Analysis of chemical equilibrium of silicon-substituted fluorescein and its application to develop a scaffold for red fluorescent probes. Anal. Chem. 2015;87(17):9061–9069.
37 Horwitz JP, Chua J, Curby RJ, Tomson AJ, Da Rooge MA, Fisher BE. et al. Substrates for cytochemical demonstration of enzyme activity. i. some substituted 3-Indolyl-β-D-glycopyranosides. Med. Chem. 1964;7(4):574-75.
38 Ho NH, Weissleder R, Tung CH. A self-immolative reporter for beta-galactosidase sensing. ChemBioChem. 2007;8(5):560-6.
39 Huang Y, Feng H, Liu W, Zhang S, Tang C, Chen J. et al. Cation-driven luminescent self-assembled dots of copper nanoclusters with aggregation-induced emission for β-galactosidase activity monitoring. J. Mater. Chem. B. 2017;5(26):5120-27.
40 Xie X, Liana Y, Xiao L, Weia L. Facile and label-free fluorescence sensing of β-galactosidase activity by graphene quantum dots. Spectrochim. Acta A Mol. Biomol. Spectrosc. 2020;240:118594.
41 Hu Q, Ma K, Mei Y, He M, Kong J, Zhang X. Metal-to-ligand charge-transfer: Applications to visual detection of β-galactosidase activity and sandwich immunoassay. Talanta. 2017;167:253-59.
42 Urano Y, Kamiya M, Kanda K, Ueno T, Hirose K, Nagano T, Evolution of fluorescein as a platform for finely tunable fluorescence probes. J. Am. Chem. Soc. 2005;127(13):4888-94.

43 Komatsu T, Kikuchi K, Takakusa H, Hanaoka K, Ueno T, Kamiya M. et al. Design and synthesis of an enzyme activity-based labeling molecule with fluorescence spectral change. J. Am. Chem. Soc. 2006;128(50):15946-47.
44 Koide Y, Urano Y, Yatsushige A, Hanaoka K, Terai T Nagano T. Design and development of enzymatically activatable photosensitizer based on unique characteristics of thiazole orange. J. Am. Chem. Soc. 2009;131(17):6058-59.
45 Egawa T, Koide Y, Hanaoka K, Komatsu T, Teraiab T, Nagano T. Development of a fluorescein analogue, TokyoMagenta, as a novel scaffold for fluorescence probes in red region. Chem. Commun. 2011;47(14):4162-64.
46 Kamiya M, Asanuma D, Kuranaga E, Takeishi A, Sakabe M, Miura M. et al. β-Galactosidase fluorescence probe with improved cellular accumulation based on a spirocyclized rhodol scaffold. J Am. Chem. Soc. 2011;133(33):12960-63.
47 Sakabe M, Asanuma D, Kamiya M, Iwatate RI, Hanaoka K, Terai T. et al. Rational design of highly sensitive fluorescence probes for protease and glycosidase based on precisely controlled spirocyclization. J. Am. Chem. Soc. 2013;135(1):409-14.
48 Doura T, Kamiya M, Obata F, Yamaguchi Y, Hiyama TY, Matsuda T. et al. Detection of LacZ-Positive cells in living tissue with single-cell resolution. Angew. Chem. Int. Ed. 2016;55(33): 9620-24.
49 Han J, Han MS, Tung CH. A fluorogenic probe for β-galactosidase activity imaging in living cells. Mol. BioSyst. 2013;9(12):3001-8.
50 Peng L, Gao M, Cai X, Zhang R, Li K, Feng G. et al. A fluorescent light-up probe based on AIE and ESIPT processes for β-galactosidase activity detection and visualization in living cells. J. Mater. Chem. B. 2015;3(47):9168-72.
51 Tseng JC, Kung AL. *In vivo* imaging of endogenous enzyme activities using luminescent 1,2-dioxetane compounds. J. Biomed. Sci. 2015;22(1):45.
52 Grimm JB, Gruber TD, Ortiz G, Brown TA, Lavis LD. Virginia Orange: A versatile, red-shifted fluorescein scaffold for single- and dual-input fluorogenic probes. Bioconjugate Chem. 2016;27(2):474-80.
53 Wei X, Hu XX, Zhang LL, Li J, Wang J. et al. Highly selective and sensitive FRET based ratiometric two-photon fluorescent probe for endogenous β-galactosidase detection in living cells and tissues Microchem. J. 2020;157:105046.
54 Calatrava-Pérez E, Bright SA, Achermann S, Moylan C, Senge MO, Veale EB. et al. Glycosidase activated release of fluorescent 1,8-naphthalimide probes for tumor cell imaging from glycosylated pro-probes. Chem. Commun. 2016;52(89):13086-89.
55 Calado RT, Young NS. Telomere Diseases. N. Engl. J. Med. 2009;361:2353-65.
56 Chatterjee SK., Bhattacharya M, Barlow JJ. Glycosyltransferase and glycosidase activities in ovarian cancer patients. Cancer Res. 1979;39:1943-51.
57 Jiang G, Zeng G, Zhu W, Li Y, Dong X, Zhang G. et al. A selective and light-up fluorescent probe for β-galactosidase activity detection and imaging in living cells based on an AIE tetraphenylethylene derivative. Chem. Commun. 2017;53(32):4505-08.
58 Yanga w, Zhaoa X, Zhanga Y, Zhouc Y, Fanb S, Shenga H. et al. Hydroxyphenylquinazolinone-based turn-on fluorescent probe for β-galactosidase activity detection and application in living cells. Dyes Pigments. 2018;156:100-7.
59 Li Y, Ning L, Yuan F, Zhang F, Zhang J, Xu Z. et al. Activatable formation of emissive excimers for highly selective detection of β-galactosidase. Anal. Chem. 2020;92(8):5733-40.
60 Huang J, Li N, Wang Q, Gu Y, Wang P. A lysosome-targetable and two-photon fluorescent probe for imaging endogenous β-galactosidase in living ovarian cancer cells. Sensor. Actuat. B-Chem. 2017;246:833-9.
61 Chen X, Zhang X, Ma X, Zhang Y, Gao G, Liu J. et al. Novel fluorescent probe for rapid and ratiometric detection of β-galactosidase and live cell imaging. Talanta. 2019;192:308-13.
62 Fu W, Yan C, Zhang Y, Ma Y, Guo Z, Zhu WH. Near-infrared aggregation-induced emission-active probe enables in situ and long-term tracking of endogenous β-galactosidase activity. Front. Chem. 2019;7:291-302.
63 Zhang X, Chen X, Zhang Y, Liu K, Shen H. et al. A near-infrared fluorescent probe for the ratiometric detection and living cell imaging of β-galactosidase. Anal. Bioanal. Chem. 2019;411:7957-66.
64 Chen M, Mu L, Cao X, She G, Shi W. A novel ratiometric fluorescent probe for highly sensitive and selective detection of β-galactosidase in living cells. Chin. J. Chem. 2019; 37(4):330-6.
65 Kong X, Li M, Dong B, Yin Y, Song W, Lin W. An ultrasensitivity fluorescent probe based on the ict-fret dual mechanisms for imaging β-galactosidase *in vitro* and *ex vivo*. Anal. Chem. 2019;91(24):15591-8.

66 Lee HW, Lim CS, Choi H, Cho MK, Noh CH, Lee K. et al. Discrimination between human colorectal neoplasms with a dual-recognitive two-photon probe. Anal. Chem. 2019;91(22):14705-11.
67 Zhaoa X, Yanga W, Fanb S, Zhouc Y, Shenga H, Caod Y. et al. A hemicyanine-based colorimetric turn-on fluorescent probe for β-galactosidase activity detection and application in living cells. J. Lumin. 2019;205:310-7.
68 Li X, Pan Y, Chen H, Duan Y, Zhou S, Wu W. et al. Specific near-infrared probe for ultrafast imaging of lysosomal β-galactosidase in ovarian cancer cells. Anal. Chem. 2020;92(8):5772-9.
69 Wu C, Ni Z, Li P, Li Y, Pang X, Xie R. et al. A near-infrared fluorescent probe for monitoring and imaging of β-galactosidase in living cells. Talanta. 2020;219:121307.
70 Pang X, Li Y, Zhou Z, Lu Q, Xie R, Wu C. et al. Visualization of endogenous β-galactosidase activity in living cells and zebrafish with a turn-on near-infrared fluorescent probe. Talanta. 2020;217:121098.
71 Long R, Tang C, Yang Z, Fu Q, Xu J, Tong C. et al. A natural hyperoside based novel light-up fluorescent probe with AIE and ESIPT characteristics for on-site and long-term imaging of β-galactosidase in living cells. J. Mater. Chem. C. 2020;8(34):11860-5.
72 Tang C, Zhou J, Qian Z, Ma Y, Huang Y, Feng H. A universal fluorometric assay strategy for glycosidases based on functional carbon quantum dots: β-galactosidase activity detection *in vitro* and in living cells. J. Mater. Chem. B 2017; 5(10):1971-9.
73 Wang W, Vellaisamy K, Li W, Wu C, Ko CN, Leung CL. et al. Development of a long-lived luminescence probe for visualizing β-galactosidase in ovarian carcinoma cells. Anal. Chem. 2017;89(21):11679-84.
74 James AL, Perry JD, Ford M, Armstrong L, Gould FK. Evaluation of cyclohexenoesculetin-beta-D-galactoside and 8-hydroxyquinoline-beta-D-galactoside as substrates for the detection of beta-galactosidase. Appl. Environ. Microbiol. 1996;62(10):3868-70.
75 James AL, Perry JD, Chilvers K, Robson IS, Armstrong L, Orr KE. Alizarin-beta-D-galactoside: a new substrate for the detection of bacterial beta-galactosidase. Lett. Appl. Microbiol. 2000;30(4):336-40.
76 Wei X, Wu Q, Zhang J, Zhang Y, Guo W, Chen M. et al. Synthesis of precipitating chromogenic/fluorogenic β-glucosidase/β-galactosidase substrates by a new method and their application in the visual detection of foodborne pathogenic bacteria. Chem. Commun. 2017;53(1):103-6.
77 Muñoz-Espín D, Serrano M. Cellular senescence: from physiology to pathology. Nat. Rev. Mol. Cell. Biol. 2014;15(7):482-96.
78 Biran A, Zada L, Karam PA, Vadai E, Roitman L, Ovadya Y. et al. Quantitative identification of senescent cells in aging and disease. Aging Cell. 2017;16 (4):661-71.
79 Lee HW, Heo CH, Sen D, Byun HO, Kwak IH, Yoon G. et al. Ratiometric two-photon fluorescent probe for quantitative detection of β-galactosidase activity in senescent cells. Anal. Chem. 2014;86(20):10001-5.
80 Zhang J, Li C, Dutta C, Fang M, Zhang S, Tiwari A. et al. A novel near-infrared fluorescent probe for sensitive detection of β-galactosidase in living cells. Anal. Chim. Acta. 2017;968:97-104.
81 Filho MS, Dao P, Gesson M, Martin AR, Benhida R. Development of highly sensitive fluorescent probes for the detection of β-galactosidase activity- application to the real-time monitoring of senescence in live cells. Analyst. 2018; 143(11):2680-8.
82 Kim EJ, Podder A, Maiti M, Lee JM, Chung BG, Bhuniya S. Selective monitoring of vascular cell senescence via β-Galactosidase detection with a fluorescent chemosensor. Sensor Actuat B-Chem. 2018;274:194-200.
83 Jiang J, Tan Q, Zhao S, Song H, Hua L, Xie H. Late-stage difluoromethylation leading to a self-immobilizing fluorogenic probe for the visualization of enzyme activities in live cells. Chem. Commun. 2019;55(99):15000-3.
84 Qiu W, Li X, Shi D, Li X, Gao Y, Li J, Mao F, Guo Y, Li J. A rapid-response near-infrared fluorescent probe with large Stokes shift for senescence-associated β-galactosidase activity detection and imaging of senescent cells. Dyes Pigments. 2020;182(99):108657.
85 Makau JN, Kitagawa A, Kitamura K, Yamaguchi T, Mizuta S. Design and development of an HBT-based ratiometric fluorescent probe to monitor stress-induced premature senescence. ACS Omega. 2020;5:11299-307.
86 Senter PD, Saulnier MG, Schreiber GJ, Hirschberg DL,Brown JP, Hellström I. et al. Antitumor effect of antibody-alkaline phosphatase conjugates in combination with etoposide phosphate. Proc. Natl. Acad. Sci. U.S.A. 1988;85(13):4842-6.
87 Senter PD, Springer CJ. Selective activation of anticancer prodrugs by monoclonal antibody-enzyme conjugates. Adv. Drug Delivery Rev. 2001;53(3):247-64.
88 Kamiya M, Kobayashi H, Hama Y, Koyama Y, Bernardo M, Nagano T. et al. An enzymatically activated fluorescence probe for targeted tumor imaging. J. Am. Chem. Soc. 2007;129(13):3918-29.

89 Gu K, Xu Y, Li H, Guo Z, Zhu S, Shi P. et al. Real-Time tracking and *in vivo* visualization of β-galactosidase activity in colorectal tumor with a ratiometric near-infrared fluorescent probe. J. Am. Chem. Soc. 2016;138(16):5334-40.
90 Tung CH, Zeng Q, Shah K, Kim DE, Schellingerhout D, Weissleder R. *In vivo* imaging of beta-galactosidase activity using far red fluorescent switch. Cancer Res. 2004;64(5):1579-83.
91 Wehrman TS, von Degenfeld G, Krutzik PO, Nolan GP, Blau HM. Luminescent imaging of beta-galactosidase activity in living subjects using sequential reporter-enzyme luminescence. Nat. Methods 2006;3(4):295-301.
92 Oushiki D, Kojima H, Takahashi Y, Komatsu T, Terai T, Hanaoka K. et al. Near-Infrared fluorescence probes for enzymes based on binding affinity modulation of squarylium dye scaffold. Anal. Chem. 2012;84(10):4404-10.
93 Zhang XX, Wu H, Li P, Qu ZJ, Tan MQ, Han KL. A versatile two-photon fluorescent probe for ratiometric imaging E. coliβ-galactosidase in live cells and *in vivo*. Chem. Commun. 2016; 52(53):8283-6.
94 Kim EJ, Kumar R, Sharma A, Yoon B, Kim HM, Lee H. et al. *In vivo* imaging of β-galactosidase stimulated activity in hepatocellular carcinoma using ligand-targeted fluorescent probe. Biomaterials. 2017;122:83-90.
95 Gnaim S, Green O, Shabat D. The emergence of aqueous chemiluminescence: new promising class of phenoxy 1,2-dioxetane luminophores. Chem. Commun. 2018;54(17):2073-85.
96 Eilon-Shaffer T, Roth-Konforti M, Eldar-Boock A, Satchi-Fainarob R. Shabat D. *ortho*-Chlorination of phenoxy 1,2-dioxetane yields superior chemiluminescent probes for *in vitro* and *in vivo* imaging. Org. Biomol. Chem. 2018;16(10):1708-12.
97 Shi L, Yan C, Ma Y, Wang T, Guo Z, Zhu WH. *In vivo* ratiometric tracking of endogenous β-galactosidase activity using an activatable near-infrared fluorescent probe. Chem. Commun. 2019;55(82):12308-11.
98 Asanuma D, Sakabe M, Kamiya M, Yamamoto K, Hiratake J, Ogawa M. et al. Sensitive β-galactosidase-targeting fluorescence probe for visualizing small peritoneal metastatic tumours *in vivo*. Nat. Comm. 2015;6:6463.
99 Zhen X, Zhang J, Huang J, Xie C, Miao Q, Pu K. Macrotheranostic probe with disease-activated near-infrared fluorescence, photoacoustic, and photothermal signals for imaging-guided therapy. Angew. Chem. Int. Ed. 2018;57(26):7804-8.
100 Li Z, Ren M, Wang L, Dai L, Lin W. Development of a red-emissive two-photon fluorescent probe for sensitive detection of beta-galactosidase *in vitro* and *in vivo*. Sensor Actuat. B-Chem. 2020;307:127643.
101 González-Gualda E, Pàez-Ribes M, Lozano-Torres B, Macias D, Wilson 3rd JR, González-López C. et al. Galacto-conjugation of Navitoclax as an efficient strategy to increase senolytic specificity and reduce platelet toxicity. Aging Cell. 2020;19(4):e13142.
102 Galiana I, Lozano-Torres B, Sancho M, Alfonso M, Bernardos A, Bisbal V. et al. Preclinical antitumor efficacy of senescence-inducing chemotherapy combined with a nanoSenolytic. J. Control Release. 2020;323:624-634.
103 Lozano-Torres B, Galiana I, Rovira M, Garrido E, Chaib S, Bernardos A. et al. An OFF–ON two-photon fluorescent probe for tracking cell senescence *in vivo*. J. Am. Chem. Soc. 2017;139(26):8808-11.
104 Lozano-Torres B, Blandez JF, Galiana I, García-Fernández A, Alfonso M, Marcos MD. et al. Real-time *in vivo* detection of cellular senescence through the controlled release of the NIR fluorescent dye Nile Blue. Angew. Chem. Int. Ed. 2020;59(35):5152-6.
105 Wang Y, Liu J, Ma X, Cui C, Deenik PR. Henderson KP .et al. Real-time imaging of senescence in tumors with DNA damage. Sci. Rep. 2019;9:2102.
106 Chen JA, Guo W, Wang Z, Sun N, Pan H, Tan J. et al. *In vivo* imaging of senescent vascular cells in atherosclerotic mice using a β-galactosidase-activatable nanoprobe. Anal Chem. 2020;92(18):12613-21.
107 Liu J, Ma X, Cui C, Wang Y, Deenik PR, Cui L. A self-immobilizing NIR probe for non-invasive imaging of senescence. 2020. bioRxiv Preprinted. doi: https://doi.org/10.1101/2020.03.27.010827
108 Aznar E, Oroval M, Pascual L, Murguía JR, Martínez-Máñez R, Sancenón F. Gated materials for on-command release of guest molecules. Chem. Rev. 2016;116(2):561–718.
109 García-Fernández A, Aznar E, Martínez-Máñez R, Sancenón F. New advances in *in vivo* applications of gated mesoporous silica as drug delivery nanocarriers. Small. 2020;16(3):1902242-304.
110 Coll C, Bernardos A, Martínez-Máñez R, Sancenón F. Gated silica mesoporous supports for controlled release and signaling applications. Acc. Chem. Res. 2013;46(2):339-49.
111 Muñoz-Espín D, Rovira M, Galiana I, Giménez C, Lozano-Torres B, Paez-Ribes M. A versatile drug delivery system targeting senescent cells. EMBO Mol. Med. 2018;10(9):e9355.